



Scholars' Mine

Masters Theses

Student Theses and Dissertations

1970

The design, construction and experimental verification of a split hopkinson bar

Woosoon Bai

Follow this and additional works at: https://scholarsmine.mst.edu/masters_theses

 Part of the [Engineering Mechanics Commons](#)

Department:

Recommended Citation

Bai, Woosoon, "The design, construction and experimental verification of a split hopkinson bar" (1970). *Masters Theses*. 5468.

https://scholarsmine.mst.edu/masters_theses/5468

This thesis is brought to you by Scholars' Mine, a service of the Missouri S&T Library and Learning Resources. This work is protected by U. S. Copyright Law. Unauthorized use including reproduction for redistribution requires the permission of the copyright holder. For more information, please contact scholarsmine@mst.edu.

THE DESIGN, CONSTRUCTION AND EXPERIMENTAL
VERIFICATION OF A SPLIT HOPKINSON BAR

BY

WOOSON BAI, 1940 -

A

THESIS

submitted to the faculty of

THE UNIVERSITY OF MISSOURI - ROLLA

in partial fulfillment of the requirements for the

Degree of

MASTER OF SCIENCE IN ENGINEERING MECHANICS

Rolla, Missouri

1970

Approved by

J. Earl Foster (advisor)

Charles J. Haas

R.D. Roche

ABSTRACT

This thesis presents the design considerations for a dynamic loading device utilizing a projectile fired from a tube. Also included is a preliminary investigation of the stress-strain relation, under dynamic loading with the device, for a plaster known as Hydrostone.

Design of the unit is based on the split Hopkinson pressure bar originally developed by Kolsky and on a similar unit in use at the Lawrence Radiation Laboratory, Livermore, California.

The strain pulses along the pressure bars are sensed by resistance wire strain gages and displayed on an oscilloscope. The oscilloscope traces are photographed and manually digitized for insertion into a computer program which gives results in terms of specimen stress, strain and strain rate. The recorded information applied for times of the order of 100 microseconds.

All equations in this thesis are based on the one-dimensional theory of stress wave propagation. Further, the material tested is shown to be reasonably isotropic and homogeneous.

The design of the loading device and attendant instrumentation has proven to be successful. Experiments were conducted on 1100-0 aluminum samples and Hydrostone plaster. Curves of results are included in the work.

ACKNOWLEDGEMENTS

The author wishes to extend his sincere thanks and appreciation to Dr. J. Earl Foster, his advisor. He also wishes to acknowledge the efforts of Dr. Charles J. Haas, for his guidance and encouragement. Finally, the author sincerely appreciates the financial support for his work under the Department of Defense contract DACA-45-69-C-0087 directed by Dr. George B. Clark of the Rock Mechanics and Explosives Research Center.

TABLE OF CONTENTS

	Page
LIST OF FIGURES	v
LIST OF SYMBOLS	vii
I. INTRODUCTION	1
II. REVIEW OF LITERATURE	2
III. OBJECTIVES	6
IV. DESIGN OF THE SPLIT HOPKINSON BAR	7
A. Air gun10
B. Velocity detector14
C. Driver and receiver bars14
D. Recoil system17
E. Electronic units17
V. HOPKINSON BAR CHARACTERISTICS AND ANALYTICAL CALCULATIONS31
VI. PARTICULAR TEST RESULTS40
VII. CONCLUSIONS AND RECOMMENDATIONS46
VIII. APPENDIX	
A. Stress, strain and strain rate of the specimen48
B. Particular test results using 1100-0 aluminum52
IX. BIBLIOGRAPHY53
X. VITA54

LIST OF FIGURES

Figure	Page
1. Hopkinson bar as modified by Kolsky	4
2. Sketch of the general arrangement of the split Hopkinson bar	8
3. Photograph of the Hopkinson bar and instrumentation which was constructed for this project	9
4. Support V blocks for the air gun	11
5. Piping diagram for the Hopkinson bar	12
6. Breech assembly of the air gun	13
7. Physical arrangement of the Photodiode units	15
8. Support block for the photodiodes	16
9. Photograph of specimen in place	18
10. Support saddles for driver and receiver bars	19
11. Sketch of the recoil system	20
12. Arrangement of the electronic console	22
13. Trigger amplifier circuit for Hopkinson bar	23
14. Response of trigger circuit to a step input	24
15. Block diagram of bar instrumentation	25
16. Strain calibration system	26
17. Wiring connections to strain gage conditioning units	27
18. Circuit used to check frequency response of the strain measuring system	29
19. Response of strain measuring system to a step input	30
20. Sketch of specimen area showing symbols used	32
21. Diagram showing stress wave propagation in split Hopkinson bar	34

LIST OF FIGURES
(continued)

Figure	Page
22. Compressive failure of Hydrostone specimens in a universal test machine	42
23. Static stress strain diagram for Hydrostone	43
24. Preliminary test data on Hydrostone	45
25. Stress, strain and strain rate test results for 1100-0 aluminum	52

LIST OF SYMBOLS

A	cross-sectional area
A_B	cross-sectional area of the impactor
A_D	cross-sectional area of the driver bar
A_R	cross-sectional area of the receiver bar
A_S	cross-sectional area of the specimen
C	velocity of one-dimensional stress waves
E	elastic modulus
E_D	elastic modulus of the driver bar
E_R	elastic modulus of the receiver bar
F	applied force
L	length
L_B	length of the impactor
L_D	length of the driver bar
L_R	length of the receiver bar
L_S	length of the specimen
m	mass
t	time
v	velocity
v_O	velocity of impactor before impact
V_I	velocity of the front face of the specimen
V_{II}	velocity of the back face of the specimen
ϵ	strain
ϵ_1	incident (loading) strain
ϵ_2	reflected strain
ϵ_3	transmitted strain

LIST OF FIGURES
(continued)

ϵ_S	average strain in the specimen
$\dot{\epsilon}$	strain rate
$\dot{\epsilon}_S$	average strain rate in the specimen
σ	stress
σ_1	incident stress
σ_2	reflected stress
σ_3	transmitted stress
σ_S	stress in the specimen
σ_{SI}	stress on the front face of the specimen
σ_{SII}	stress on the back face of the specimen
σ_{AVG}	average stress in the specimen
ρ	density
ρ_B	density of the projectile
ρ_D	density of the driver bar
ρ_R	density of the receiver bar
ρ_S	density of the specimen

I. INTRODUCTION

The mechanical behavior of materials at very high strain rates has been investigated using the split Hopkinson bar method with one-dimensional elastic wave propagation theory. In general, the mechanical properties of materials highly depend on the rate of applied stress.

The split Hopkinson bar is well known as a dynamic loading device for intermediate strain rates. A cylindrical specimen is sandwiched between two pressure bars, one called a driver and the other a receiver. The driver bar is impacted with an impactor generating a stress wave which propagates along the driver unit. The wave is transmitted to the specimen and the receiver bar in turn. Both pressure bars remain in the elastic range throughout the test.

The strain-time histories in the pressure bars are sensed by resistance-strain gages and displayed on a memory type oscilloscope. Photographs of the oscilloscope traces are taken for a permanent record.

The analytical relations which describe the wave propagation in the Hopkinson bar are derived and included in the text. A computer program was written for calculating stress, strain and strain rate as a function of time. The code listing is in Appendix A.

II. REVIEW OF LITERATURE

The split Hopkinson bar supplies a method by which strain rate information can be obtained for the range of 10 sec.^{-1} to 1000 sec.^{-1} . Conventional, universal testing machines have an upper limit of approximately 10 sec.^{-1} while slap plate tests (1)* produce rate information above the range of the Hopkinson bar by an order of magnitude or more. For the intermediate range, however, the Hopkinson bar is the only device at the present time that gives the desired information.

The history of this type of testing is long and varied. Hopkinson (2), in 1914, developed an apparatus now known as the Hopkinson pressure bar which consisted of a cylindrical steel bar with a pellet lightly attached on one end. The device was used to investigate the pressure-time relation for a pulse generated by means of an impact with the bar. The complete unit was suspended as a pendulum.

The compressive pulse propagated along the bar, through the pellet and reflected from the free face of the pellet as a tensile wave. When the reflected wave reached the interface between the pellet and bar, the pellet "flew off" and was later caught in a ballistic pendulum. By momentum principles the velocity of the pellet could be determined. Although this method gives a series of integrated pressure-time values, the actual pressure-time relation of the incident pulse cannot be determined uniquely by this procedure if the pulse has a relatively long rise time. Further, the method is not practical in measuring pulses of small amplitude.

* Numbers in parantheses refer to the Bibliography at the end of the thesis.

Davies (3), in 1948, overcame the two disadvantages mentioned above by installing a capacitance gage at the end of the bar instead of the pellet. He obtained a continuous record of the minute displacements of the free end of the bar and was able to discern the excitation strain pulse. He also investigated the theory of the propagation of pulses along cylindrical bars and specifically the limitations imposed by geometric dispersion.

Kolsky (4), in 1949, further modified the Hopkinson experiment by inserting a thin specimen between the driver bar and the receiver bar as shown in figure 1. The modification has been universally adopted and in the process has considerably enhanced Professor Kolsky's esteem in the scientific community.

The device as shown in figure 1 consists of two long high-strength cylindrical bars hereafter called the driver and receiver bar. Throughout the test the stresses in the driver and receiver units remain in the elastic range while the specimen can respond plastically. The principle of the method is that the incident compressional pulse will reflect from the specimen-driver interface and a wave will be transmitted through the specimen into the receiver bar. Strain readings are taken from the driver and receiver units and from these data the response within the specimen can be calculated.

Other authors have contributed by using the split Hopkinson bar. Maiden and Green (5), in 1966, presented strain-rate tests on the specimens of 6061-T6 aluminum, 7075-T6 aluminum, pyrolytic graphite, lucite, and micarta at strain rates from 10^{-3} to 10^4 sec.⁻¹, using a variety of strain-rate machines including the split Hopkinson bar. Lindholm and Yeakley (6), in 1968, presented details for obtaining complete

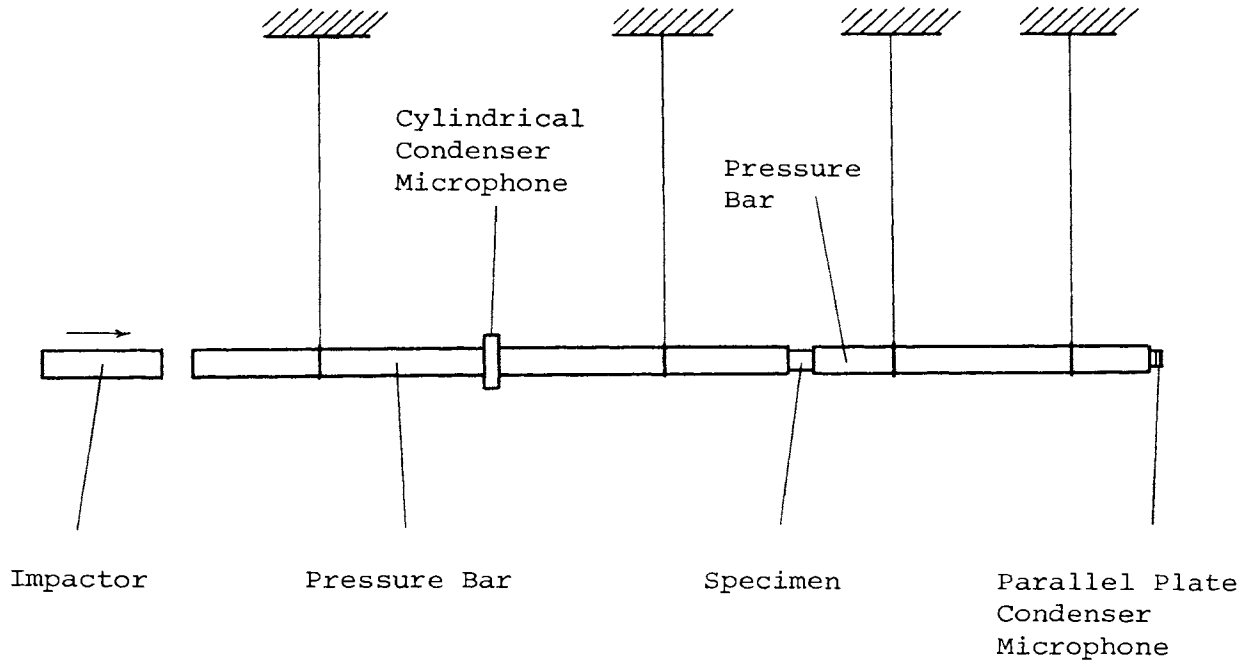


Figure 1. Hopkinson Bar as Modified by Kolsky.

stress-strain curves at strain rates on the order of 10^3 sec.^{-1} in either tension or compression with 1100-0 aluminum. Rand and Jackson (7), in 1967, demonstrated analytically that although the presence of axial inertia does cause nonuniform distribution of stress, strain and rate of strain, the various averaging processes result in a reasonable approximation of the actual stress-strain relation. Also, their experimental studies indicate that the effects of friction and radial inertia are negligible.

Ricketts and Goldsmith (8), in 1970, presented the response of natural rocks and concrete-like composites to dynamic loading using the Hopkinson bar suspended as a pendulum. They also analyzed the data from the point of view of dissipation and dispersion with the objective of establishing dynamic constitutive equations. The results indicated that some rocks exhibited virtually no change in pulse shape, while more attenuation was observed in volcanic materials. No noticeable alteration in pulse shape was observed in these latter materials.

III. OBJECTIVES

For some time the Rock Mechanics and Explosives Research Center has felt the need for a dynamic loading device such as the split Hopkinson bar. Recently a THEMIS contract was awarded the Center under which fundamental properties of all types of rock and rock-like materials were to be studied. One of the areas mentioned in this contract was intermediate rate effects, thus past need became an immediate requirement. It was with this incentive that the bar was constructed.

The objective of this report is to present the design which was followed together with test results for one material. Also included are a summary of the equations and a computer program used in the analysis of the data.

IV. DESIGN OF THE SPLIT HOPKINSON BAR

The intermediate-rate-effect device consists of five principal parts which are listed below. A sketch of the arrangement is shown in figure 2. Where possible, nonmagnetic materials were used in the construction of the unit.

The components are

- A. Air gun
 - 1. Gun barrel
 - 2. Compressed air supply unit
 - 3. Vacuum unit
- B. Velocity detector
- C. Driver and receiver bars
- D. Recoil system
- E. Electronic units

Most of the component parts are firmly attached to a wood table specially constructed for this purpose. A photograph of the installation is shown in figure 3. The table has a 3/4 in. plywood top supported by ten, 4 in. by 4 in. legs which are equipped with levelling screws. The table height is 34 in. from the floor. An aluminum channel, 4 in. in depth and 24 ft. in length, is bolted to the plywood top of the table. Care was taken to level the channel to present a flat surface for support of other mounted parts.

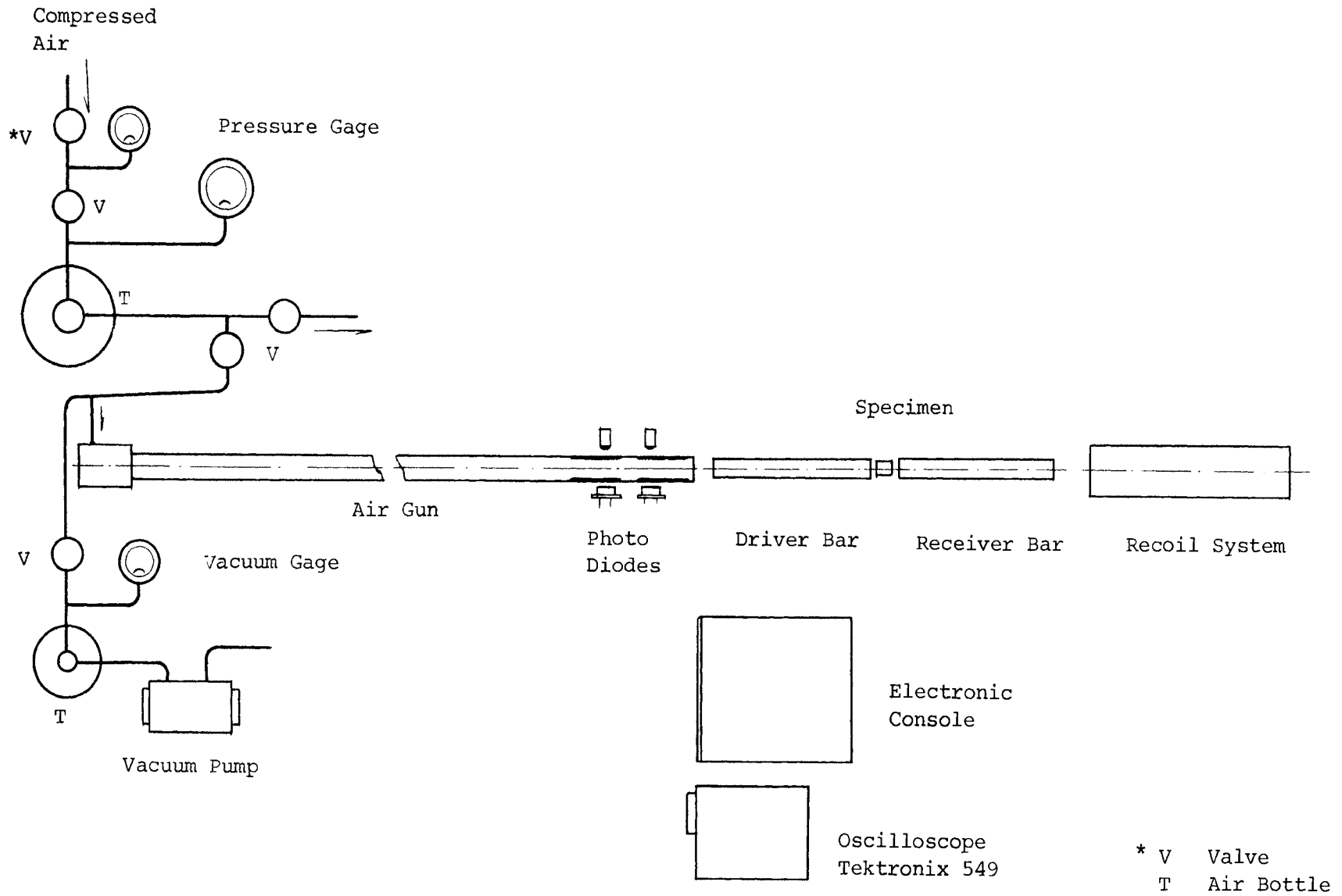


Figure 2. Sketch of the General Arrangement of the Split Hopkinson Bar

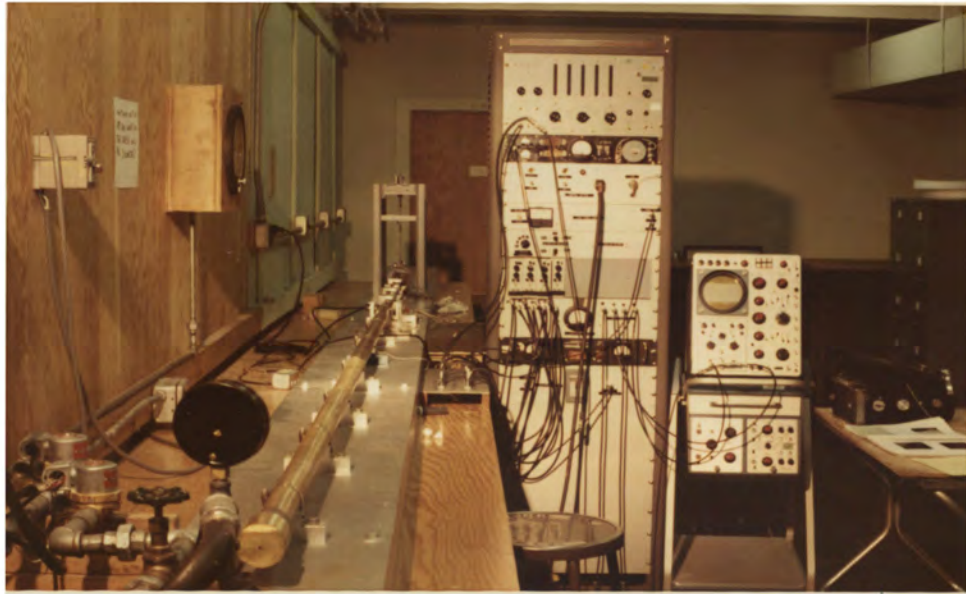


Figure 3. Photograph of the Hopkinson Bar and Instrumentation which was Constructed for this Project.

A. Air gun

A brass tube, 12 ft. in length and 1.49 in. ID, constitutes the barrel of the air gun. The complete unit is mounted on V blocks (figure 4) which are bolted to the channel. A surveyor's transit was used to align the V blocks and ordinary automobile hose clamps were used to secure the tube to the blocks.

A schematic diagram is shown in figure 5 in which significant parts are labelled. The laboratory compressed-air supply (of approximately 90 psi) is taken from the supply main through a cut-off valve, V_1 , a solenoid valve, V_2 , to a compressed air bottle, T_1 , which acts as a storage reservoir. To fire the gun, solenoid valve, V_3 , is opened with a key switch on the control console. Air is directed from T_1 through V_3 to the gun barrel, the pressure acting to force the impactor down the tube. The initial firing pressure is controlled by monitoring the pressure gage, G_2 , which is mounted on a wall near the console. A solenoid dump valve, V_4 , can be actuated to bleed the system if desired.

To cock the gun the projectile is returned to the breech by use of a vacuum system. A pump is used to evacuate a second air bottle T_2 ; then, when desired, valve V_5 is cracked to create a vacuum in the gun barrel. Atmospheric pressure then forces the impactor to return to the starting position. A rubber bumper is installed in the breech to cushion projectile impact at the head of the tube. The breech assembly is shown in figure 6.

Regarding piping sizes, either 1/4 in. or 3/4 in. was used throughout the system. A 3/4 in. flexible hose was used between the air bottle, T_1 , and the assembly mounted on the table. The vacuum bottle,

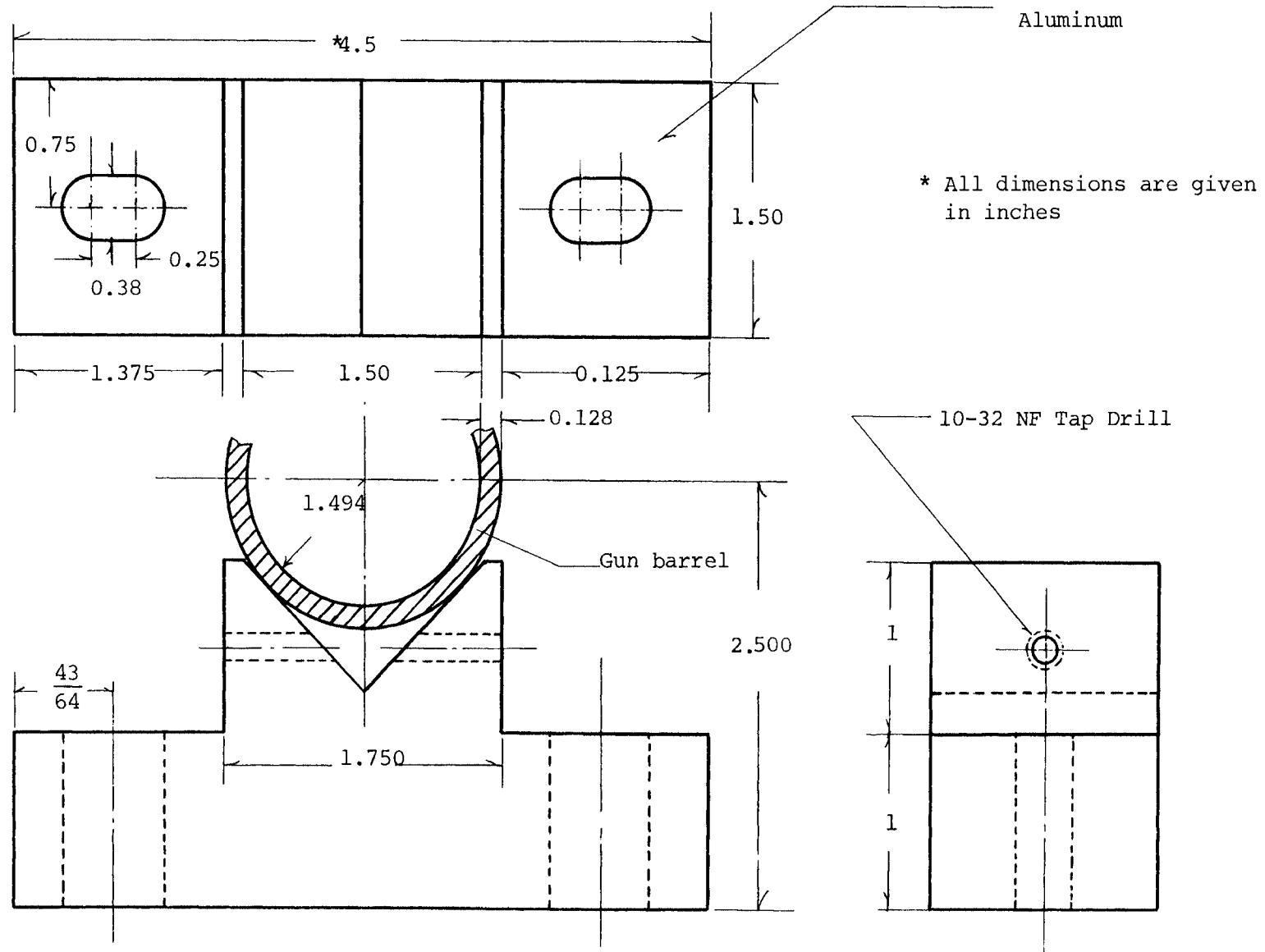
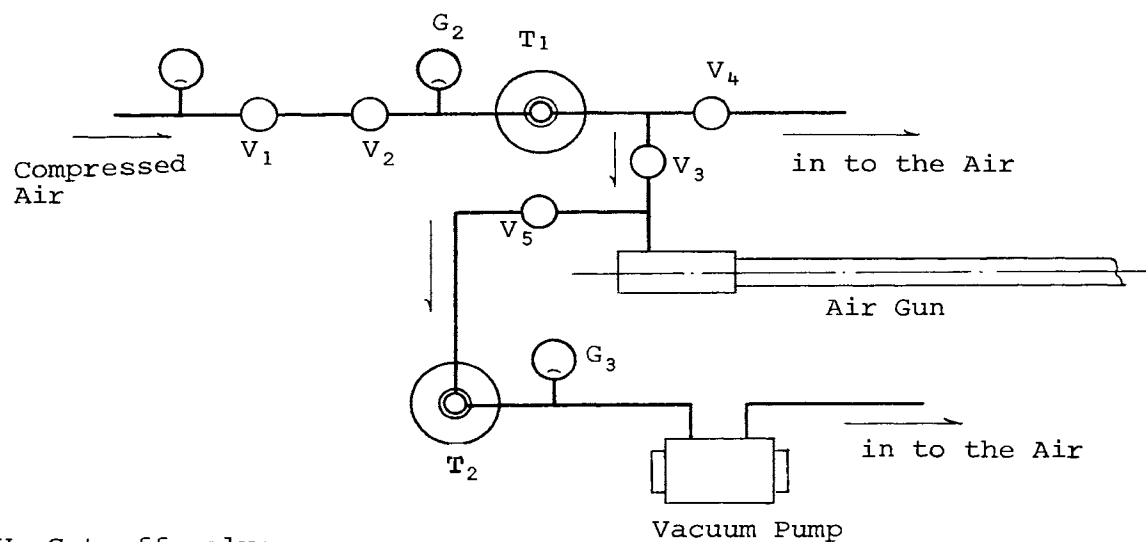


Figure 4. Support V-Blocks for the Air Gun.



- V₁ Cut off valve
- V₂ Solenoid valve
- V₃ Solenoid valve
- V₄ Solenoid dump valve
- V₅ Valve
- G₂ Pressure gage
- G₃ Pressure gage
- T₁ Air bottle
- T₂ Air bottle

Figure 5. Piping Diagram for the Hopkinson Bar.

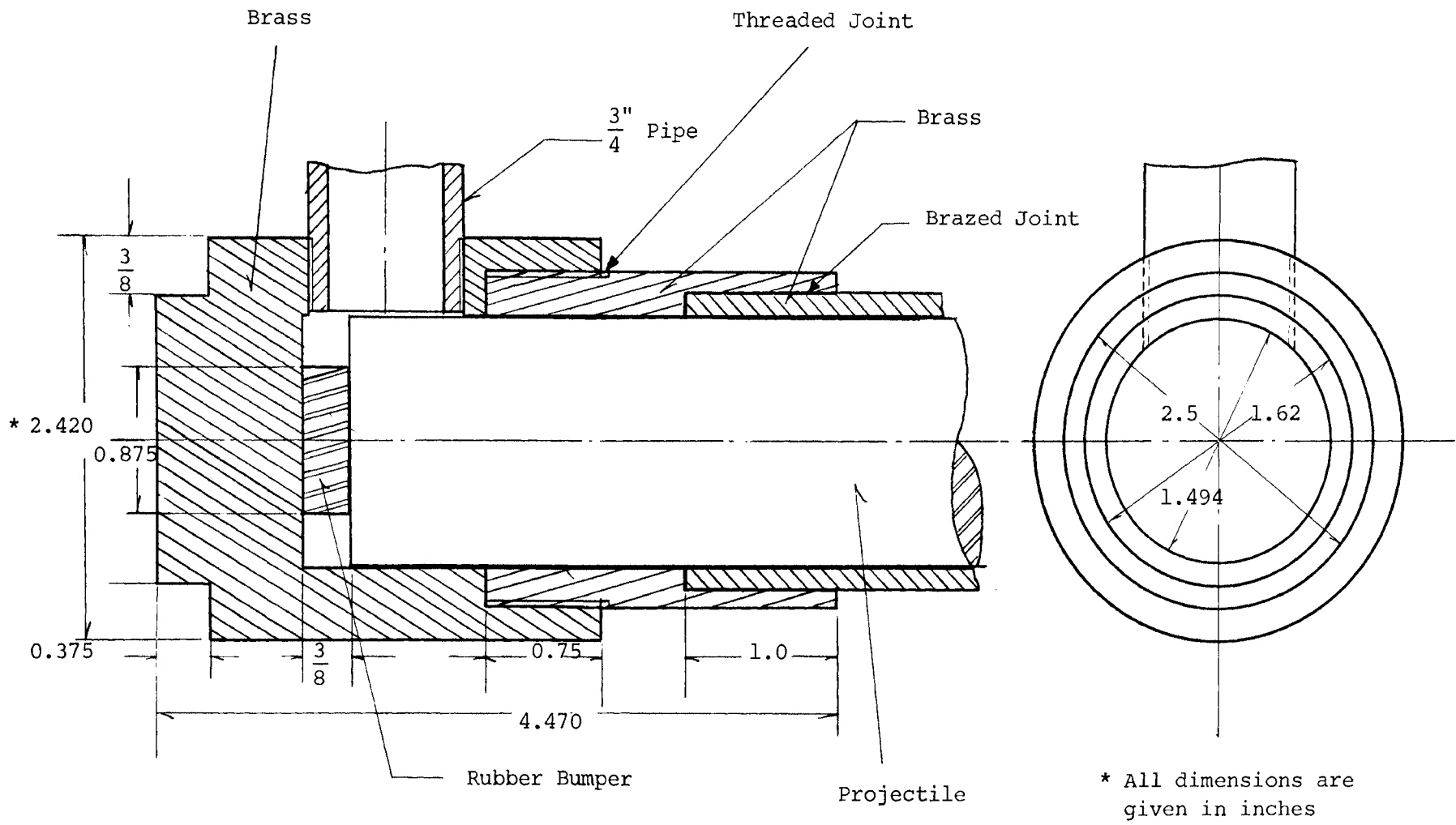


Figure 6. Breech Assembly of the Air Gun.

T₂, was connected to the vacuum pump in the same manner with 1/4 in. hose. Laboratory air was led to the air bottle, T₁, with 1/4 in. pipe but to reduce friction and choking effects, the 3/4 in. size was used between the bottle and the gun.

B. Velocity detector

Just prior to impact at the test end of the tube the velocity of the projectile is detected with two light sources and associated photo-cells spaced a known distance apart. Four slots were milled in the gun barrel in this area such that the two light beams could span the tube diameter. The light beams are turned on before the test and are subsequently interrupted by the projectile. As the projectile breaks the first beam a counter is triggered to begin counting a 100 KC oscillator in a Hewlett Packard Model 522B electronic counter until stopped by the action of the projectile cutting the second beam. With this method time intervals can be measured in milliseconds to two decimal places.

The physical arrangement is shown in figure 7 which indicates the two light sources on one side of the tube and the two photodiode receivers on the opposite side. Supporting blocks for the two units are shown in figure 8. It should be noted that each source-receiver unit is mounted on a single block to maintain a constant distance between them. The circuit diagrams for the lamps, photodiodes, and trigger amplifier are discussed in section E of this chapter.

C. Driver and receiver bars

Data output from the split Hopkinson bar is obtained from strain gages mounted on the driver and receiver bars. These two units are 2 ft. long, 1.122 in. in diameter and are made from 7075-T6 aluminum. Two strain gages (Micro-Measurements, type ED-DY-BG-350) are attached

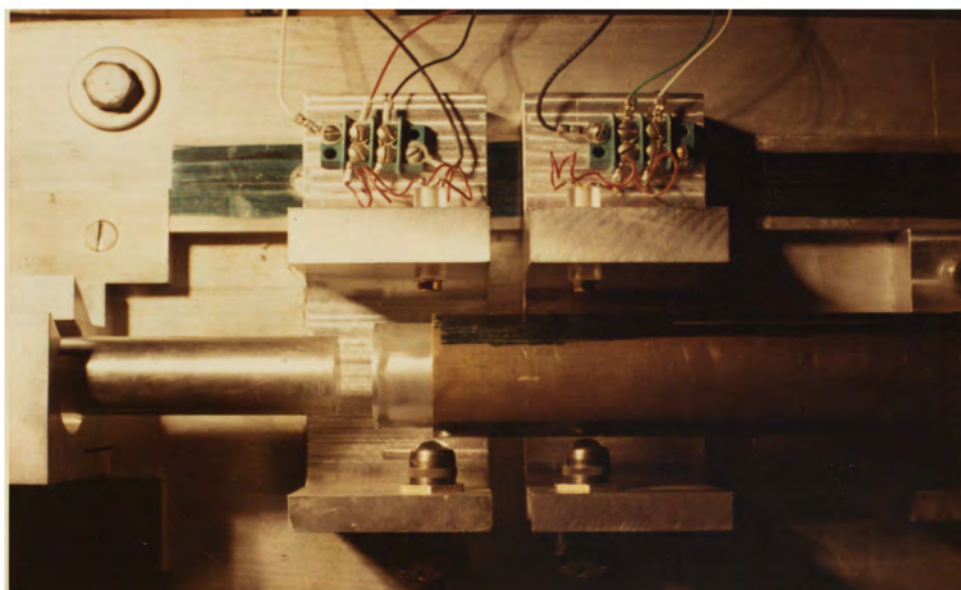
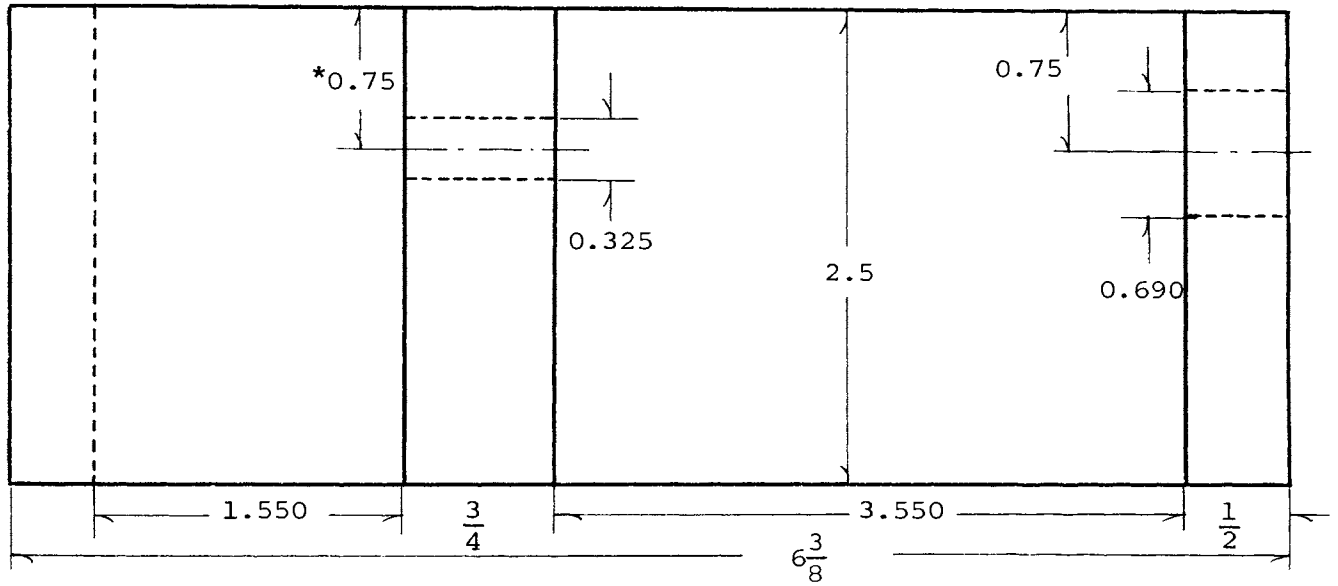


Figure 7. Physical Arrangement of the Photodiode Units.



* All dimensions are given in inches

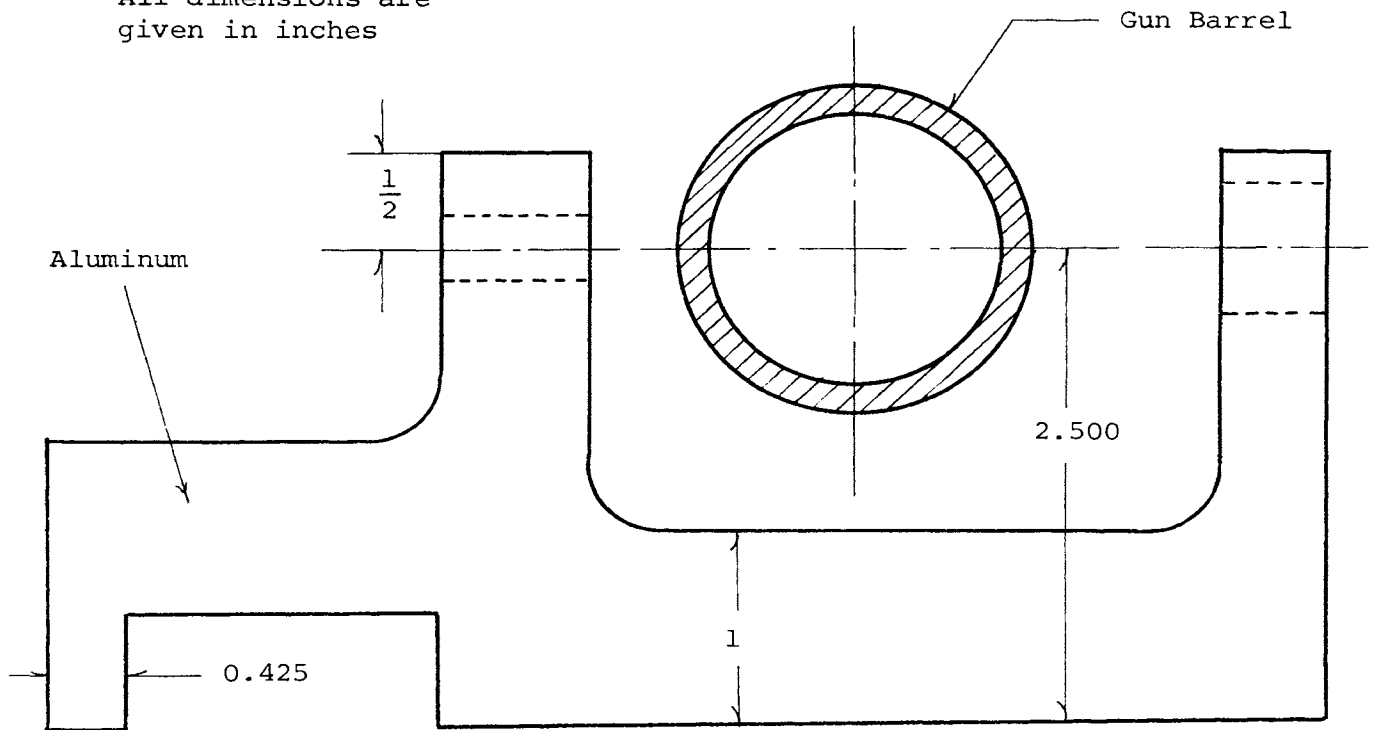


Figure 8. Support Blocks for the Photodiodes.

to each bar with Baldwin-Lima-Hamilton EPY-150 Epoxy cement. The gages are located 7.0 in. from the specimen and are mounted in a longitudinal direction and diametrically opposite each other. All gage units were initially checked by loading the bars statically in a universal testing machine. A photograph of the specimen area is shown in figure 9.

Aluminum "saddles" were designed as shown in figure 10 to support the bars on the channel. Three adjusting screws are located around the bar diameter at 120 degree angles. These screws are tipped with Teflon points to reduce surface friction to a minimum and are adjusted to give precise alignment of the driver and receiver bars with the axis of the gun barrel.

D. Recoil system

A weight-pendulum type of recoil system was designed and constructed to absorb the energy imparted to the system by the projectile. A sketch of the unit is shown in figure 11. The device consists of a lead billet, 4 in. in diameter and 16 in. in length suspended from the support structure by two pendulum arms. Upon impact by the receiver bar, the lead block moves in curvilinear translation. When the billet deflects through the maximum angle and starts to return, a ratchet-pawl system locks it in the deflected position. In this way the incident energy of the impactor is converted to potential energy of the billet.

E. Electronic units

All electronic units are housed in the control console except the triggering circuits which are located on the table with the Hopkinson bar. These consist of an electronic counter (Hewlett Packard Model 522B) for measuring projectile impact velocity, B&F strain gage

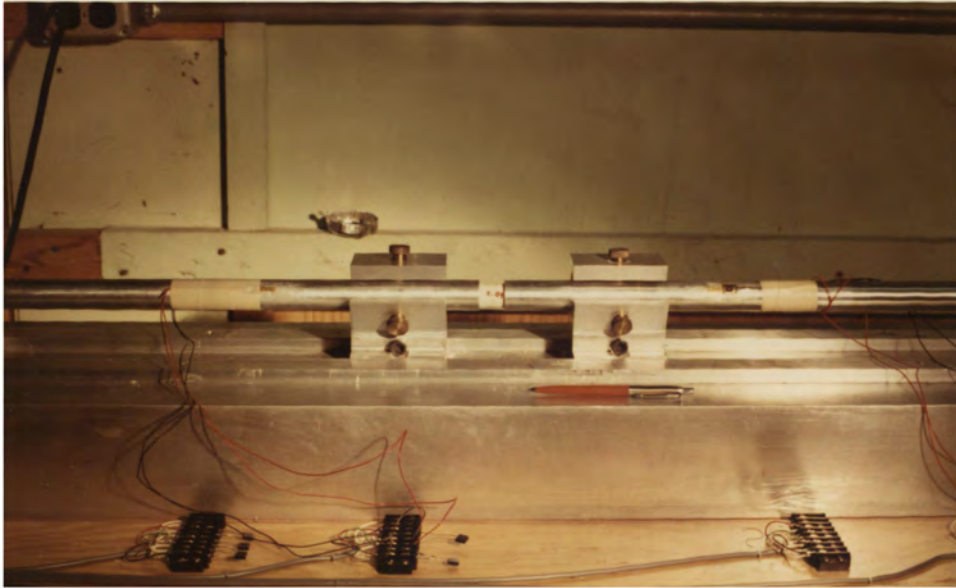


Figure 9. Photograph of Specimen in Place.

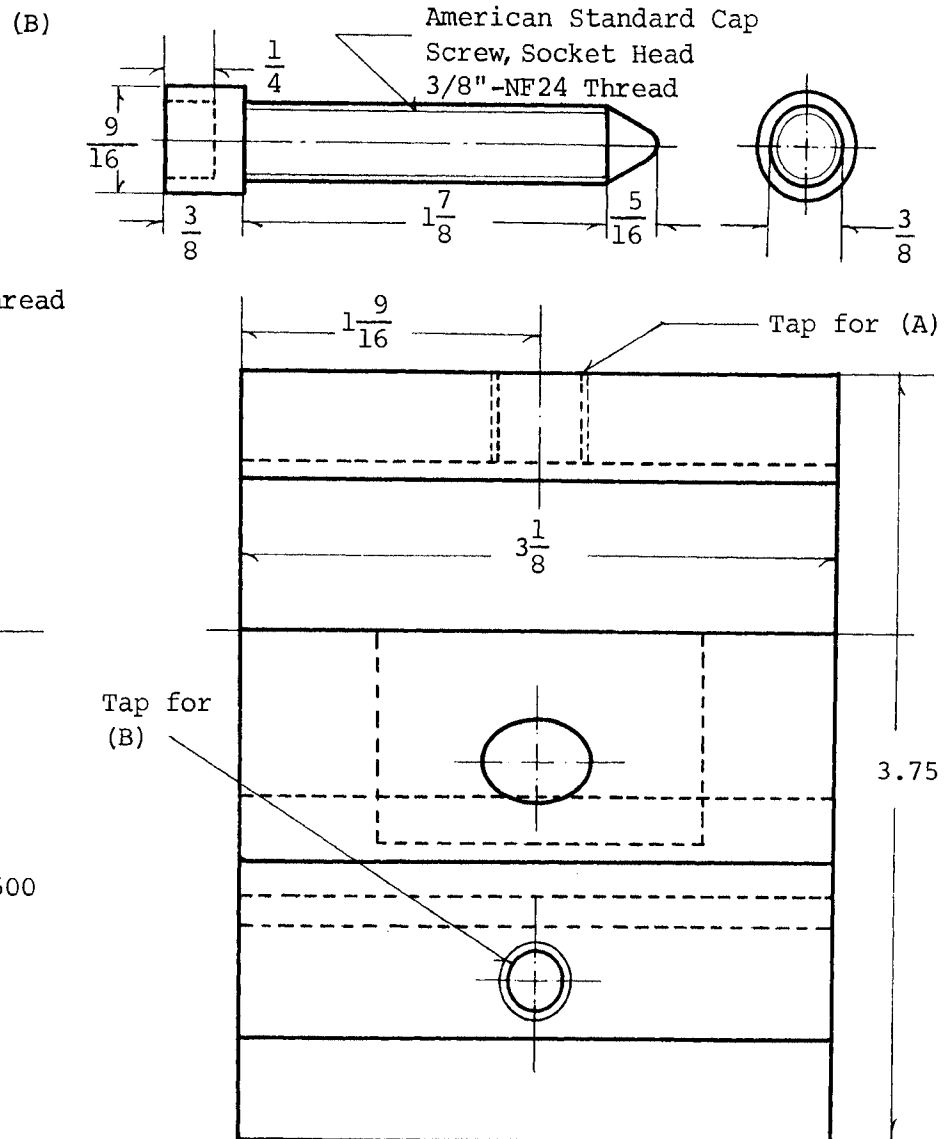
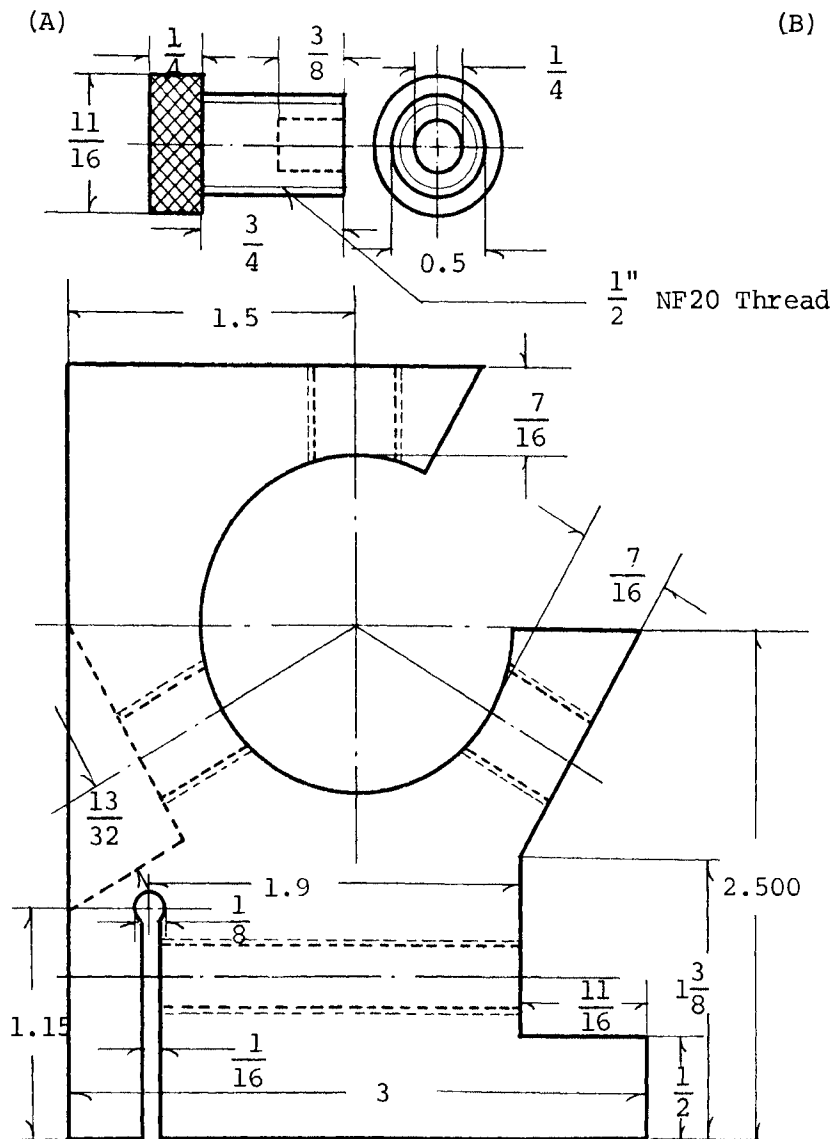


Figure 10. Support Saddle for Driver and Receiver Bars.

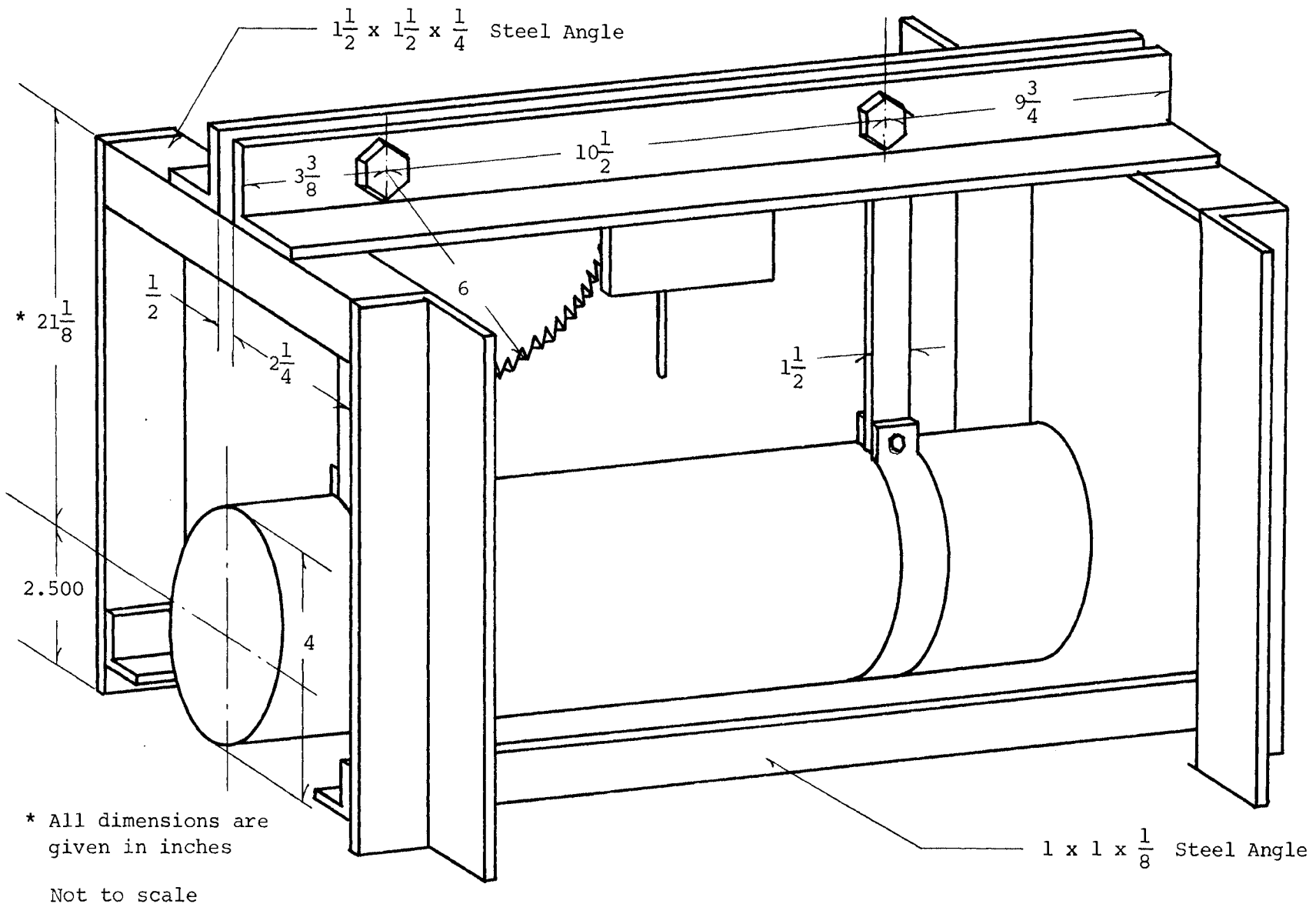


Figure 11. Sketch of the Recoil System.

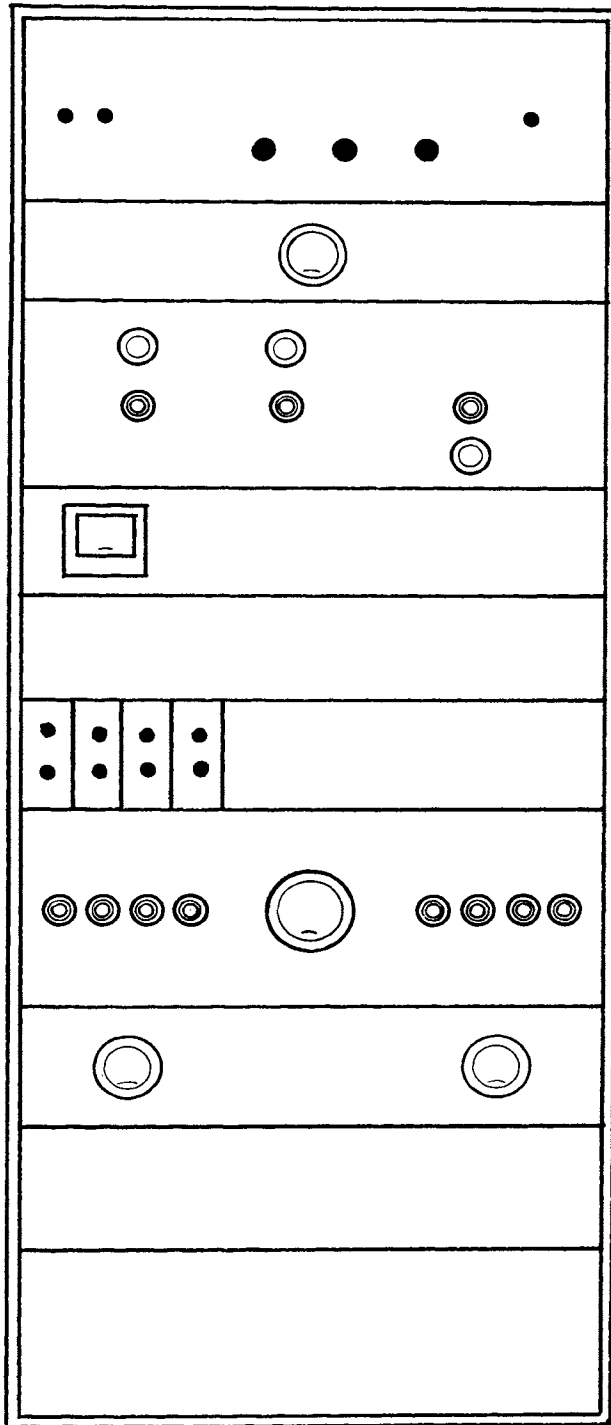
conditioning units, power supplies and control circuits. A sketch of the control console is shown in figure 12.

The trigger amplifier circuitry for starting and stopping the counter consists basically of two photodiode units which actuate two flip-flops as shown in figure 13. A flip-flop circuit is one which can exist indefinitely in either of two stable states and can be induced to make an abrupt transition from one state to the other by means of external excitation. One flip-flop is used to start the counter when the first light beam has been broken and the other is used to stop the unit when the second light beam has been interrupted.

A flip-flop with 0.5 μ sec. rise time was used to trigger the counting system to determine the response of the associated circuitry. The trigger pulse shown in figure 14 indicates that the rise time is approximately 3.5 μ sec. Since the counter triggers in the low microsecond range and the time interval being measured to compute velocity is on the order of 10 msec., the response of the counting circuit can be considered instantaneous. Accurate measurement of time interval is therefore assured.

The oscilloscope can be triggered from either of the photocells as shown in figure 15. Another means is based on the driver bar being insulated from ground by teflon riders. When the projectile strikes the driver bar the oscilloscope can be triggered by shorting the bar to ground through the projectile.

The calibration network consists of several precision calibration resistors and switches so that any individual calibration resistor can be shunted across one of the inactive arms of the bridge circuit as shown in figures 16 and 17. The B&F strain gage conditioning units are wired to accept a four arm external bridge. Normally the system



Electronic Counter
Hewlett Packard
Model 522B

Power Supply (-12V DC)
Bias for Trigger Amp.

Control Switches

Lamp Power Supply
(+12V DC)

Shunt Resistance
Calibration Network

B&F Strain Gage
Conditioning Units

Connector Unit

Power Supply +24V DC
B⁺ for Trigger Amp.

Main Power Switch &
Connector for -24V DC

Blank

Figure 12. Arrangement of the Electronic Console.

* R₁ 470K
 R₂ 3.5K
 R₃ 2.43K
 R₄ 1K
 R₅ 10K

R₆ 100K
 C₁ 0.001μf
 P_d Photo Diode
 No. SGD-100A
 (EG&G)

All resistors are of ½ watt unless specified
 All transistors are TRW 6729 unless specified
 All Zener diodes 7 Volt 200 milliamp
 All diodes are GE General Purpose 200 milliamp

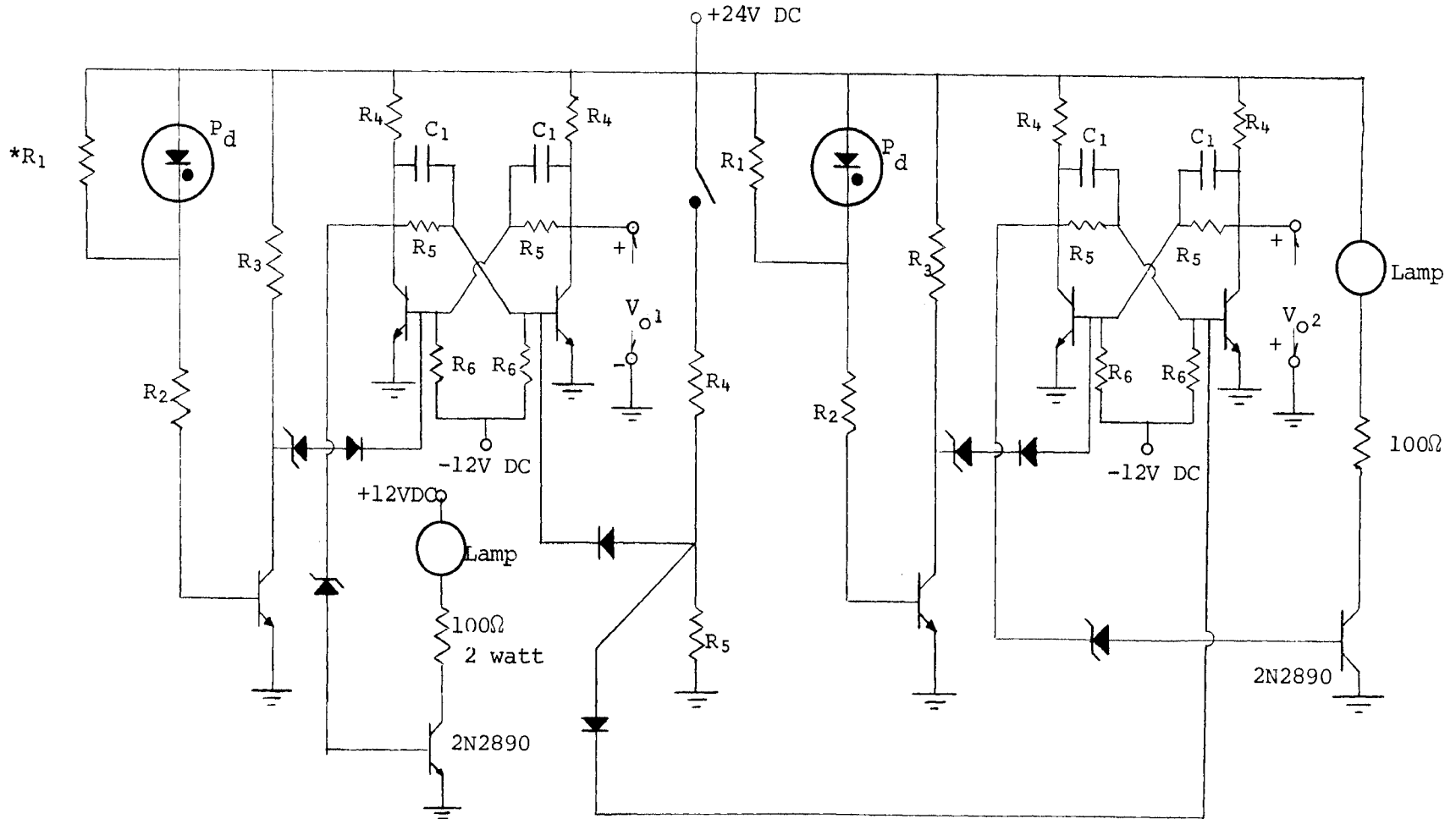
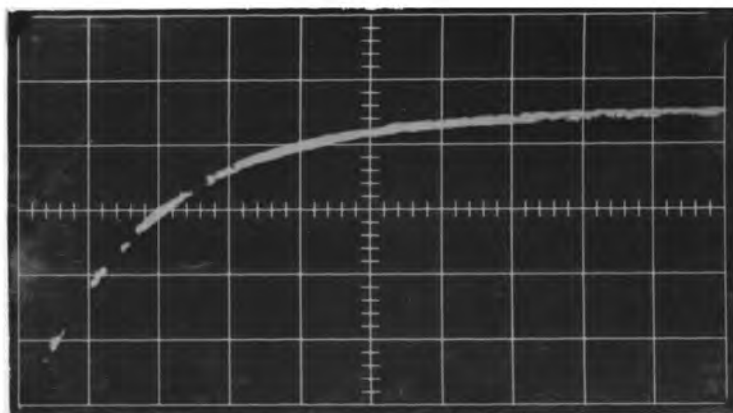


Figure 13. Trigger Amplifier Circuit for Hopkinson Bar.



Vertical Scale 5 volts/cm.
Horizontal Scale 1 μ sec./cm.

Figure 14. Response of Trigger Circuit to a Step Input.

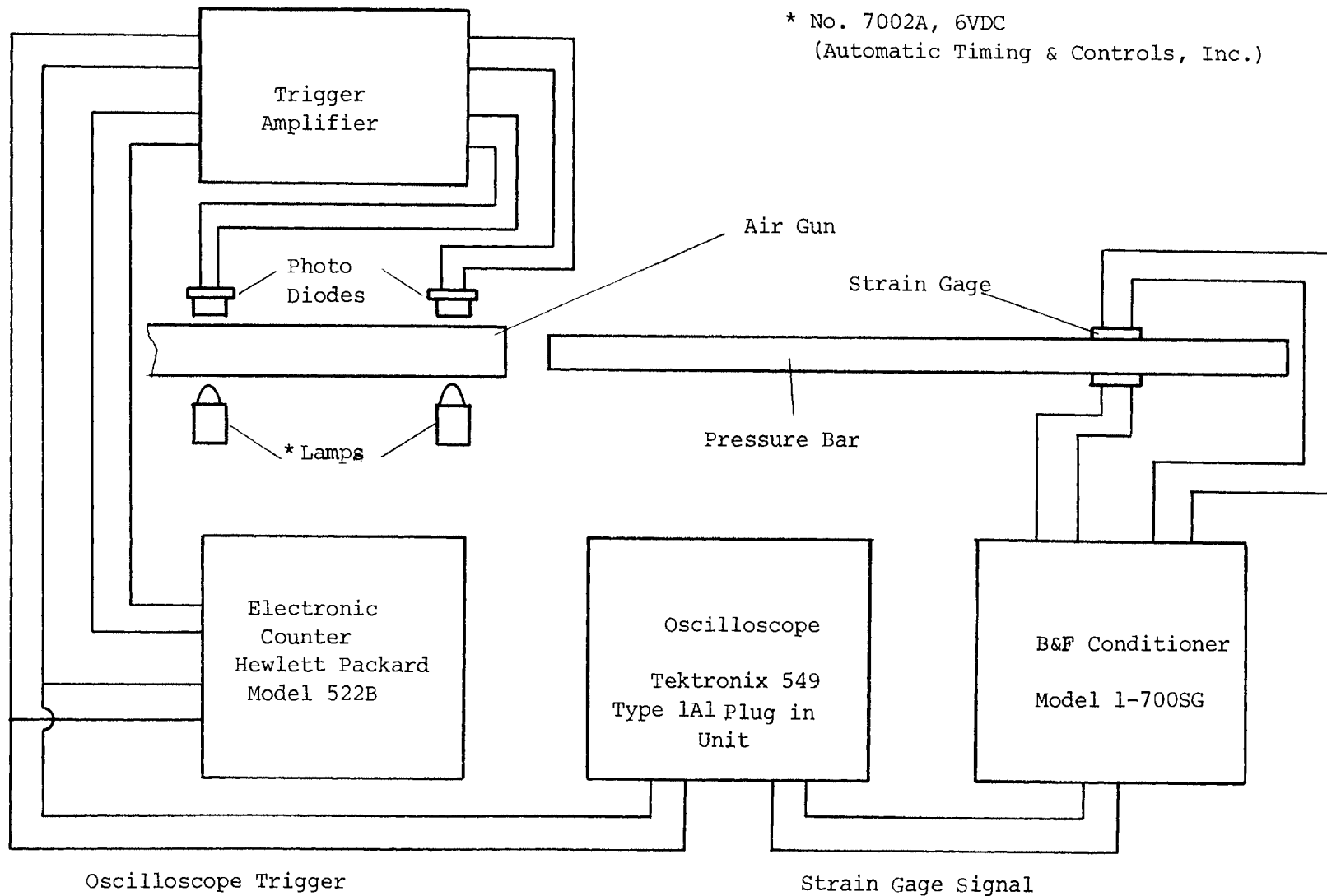


Figure 15. Block Diagram of Bar Instrumentation.

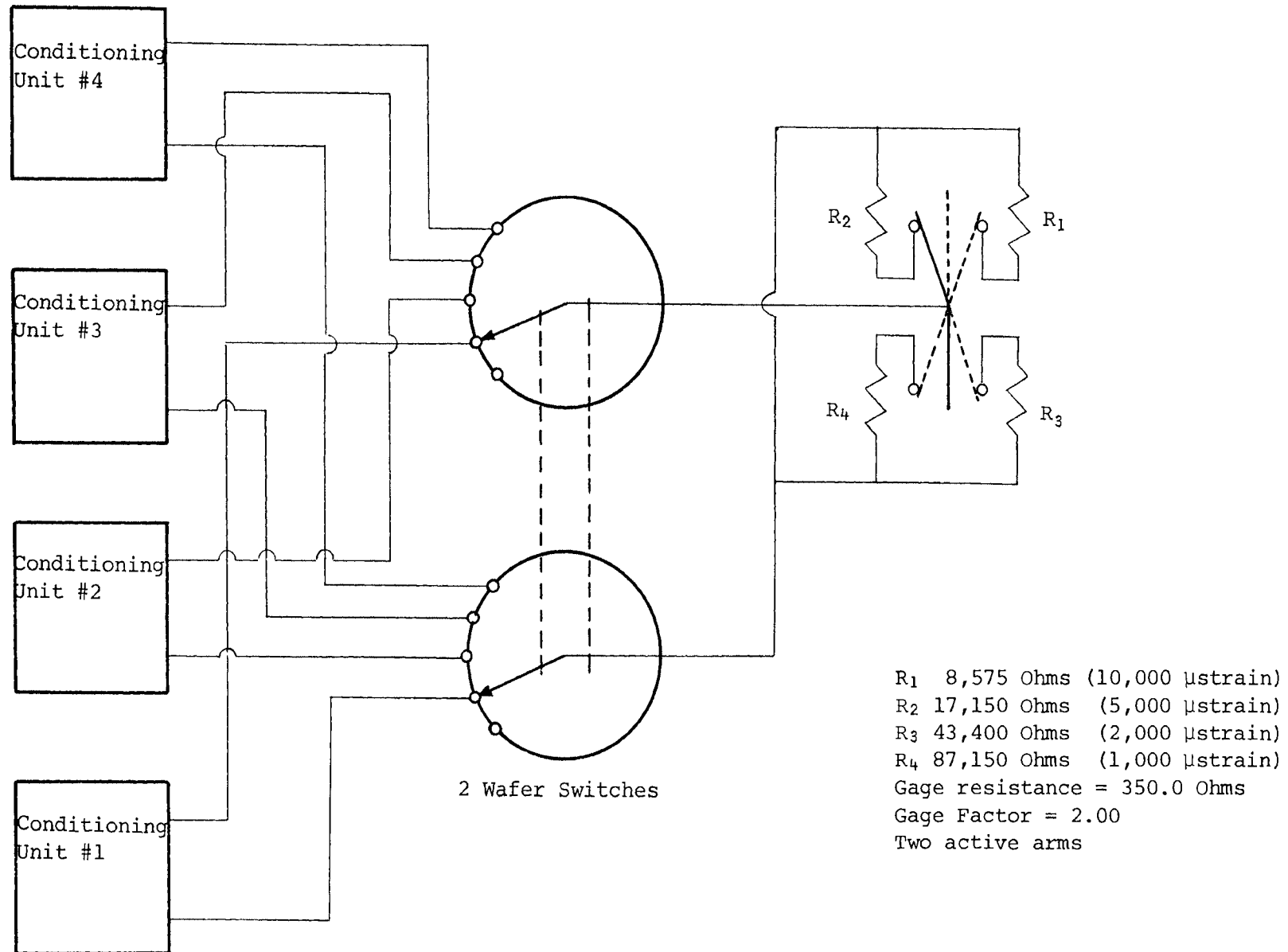


Figure 16. Strain Calibration System.

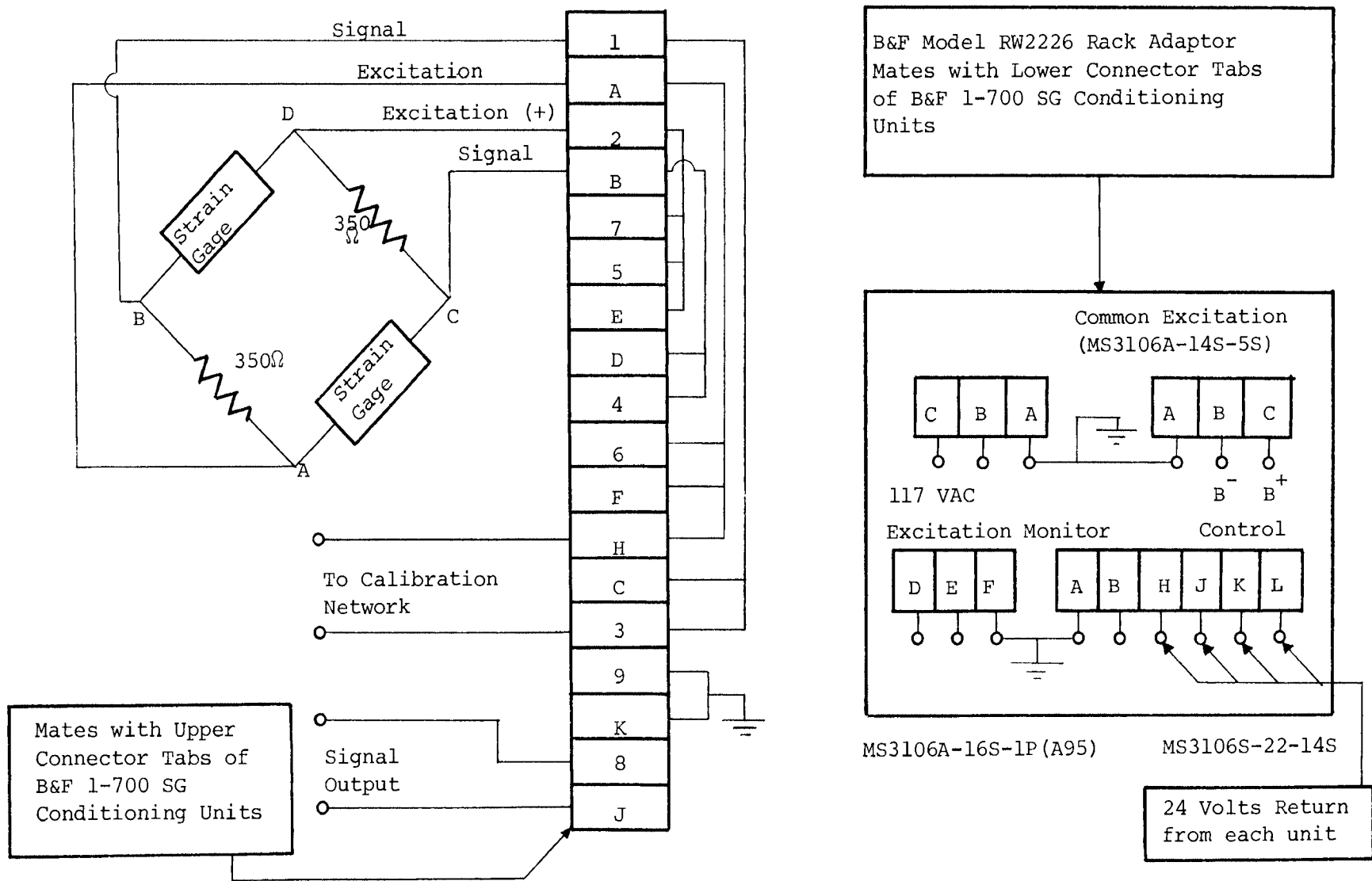


Figure 17. Wiring Connections to Strain Gage Conditioning Units.

is operated with two active arms (both compression) and with two bridge completion resistors located on the table near the strain gages. In this way maximum noise cancellation is obtained.

The following procedure was used to check frequency response of the entire strain measuring system.

An astable multivibrator was used to drive a transistor between cut-off and saturation. When in saturation, a short circuit (with proper considerations) will exist between the collector and the emitter and when in cut-off a very high impedance will exist between these two elements. The amount of current driven into the base will determine the state of the transistor. The diagram of the circuit is shown in figure 18.

To test response, a resistor, placed in parallel with one arm of the bridge, is switched in and out at a very fast rate. This will give a periodic unbalance to the bridge at the multivibrator frequency. The results of the test are shown in figure 19 parts (a) and (b). The response of the test circuitry is shown in part (a) and it is seen that the resistor is switched into the circuit in approximately $0.3 \mu\text{sec}$. System response is given in part (b) wherein the lower trace shows a rise time of approximately $0.6 \mu\text{sec}$. when the signal is fed directly into the Tektronix Type 1A1 plug in unit and the upper trace shows the effect of a particular preamplifier which is sometimes used. Based on these results the system is deemed adequate to record the type of stress pulses that will be experienced with the Hopkinson bar.

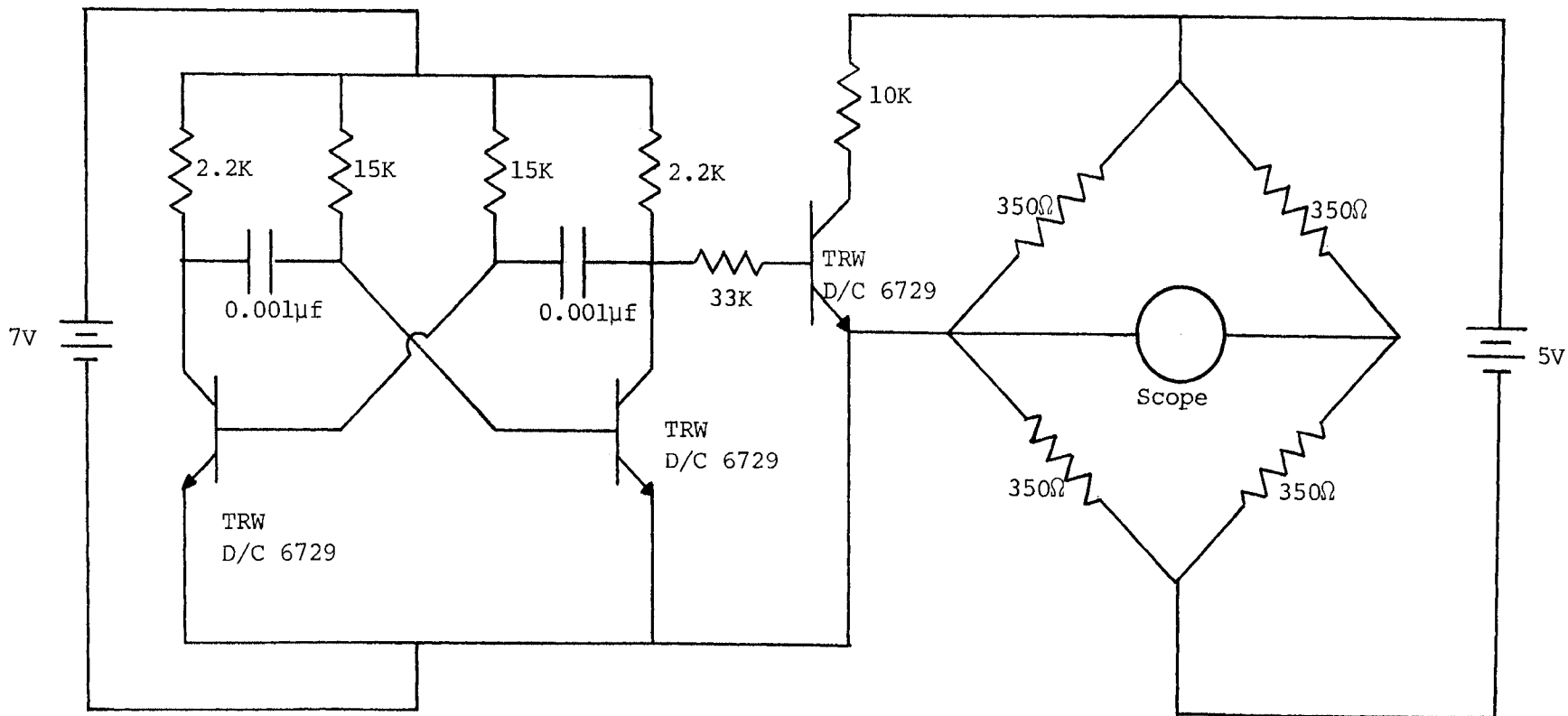
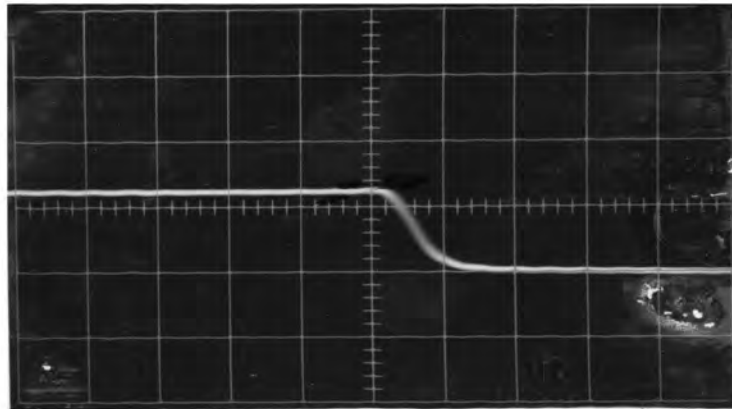
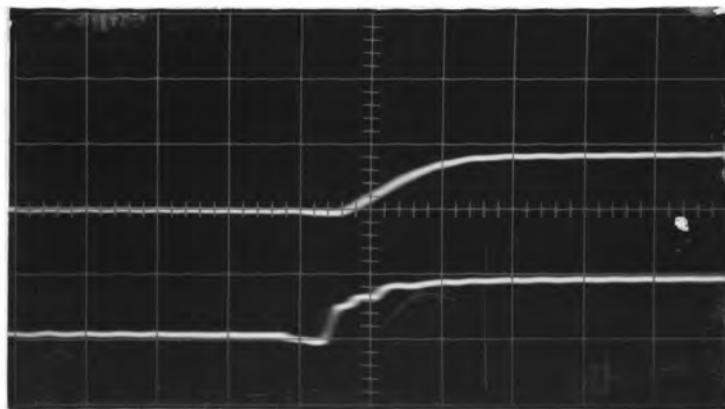


Figure 18. Circuit used to Check Frequency Response of the Strain Measuring System.



(a) Vertical Scale 2 volts/cm.
Horizontal Scale 0.4 μ sec./cm.



(b) Vertical Scale 0.05 volts/cm.
Horizontal Scale 0.4 μ sec./cm.

Figure 19. Response of Strain Measuring System to a Step Input.

V. HOPKINSON BAR CHARACTERISTICS AND ANALYTICAL CALCULATIONS

The specimen to be investigated was sandwiched between two aluminum cylindrical pressure bars as shown in figure 9. Lengths of the bars were made long to extend signal recording time. Signals are useable until complicating reflections occur from the free ends of the receiver bar and the projectile.

Two resistance strain gages were mounted on the driver and receiver bars at a distance of 7.0 in. from the specimen interface. This follows the procedure of recording from a position of at least 5 diameters from the impact surface. A sketch of the arrangement is shown in figure 20. The pressure bars were also made larger in diameter than the specimen to allow for radial expansion of the specimen during impact.

The following assumptions were made for the test analysis:

1. The driver and receiver bars remain elastic throughout the test.
2. The pressure pulse is propagated without geometric dispersion. This assumption is only true provided the wave lengths comprising the pulse are large compared with the lateral dimension of the bars.
3. The stress pulses are uniformly distributed over the cross section of the bars.
4. After several wave reflections within the specimen, a uniaxial state of stress will exist and the stress, strain and strain rate will assume nearly constant values over the length.

The diameter of the specimen should be relatively small so that radial inertia forces do not significantly influence the stress state. Further the length of the test specimen should be short enough to allow accurate averaging of the stresses at each interface.

* All dimensions are given in inches

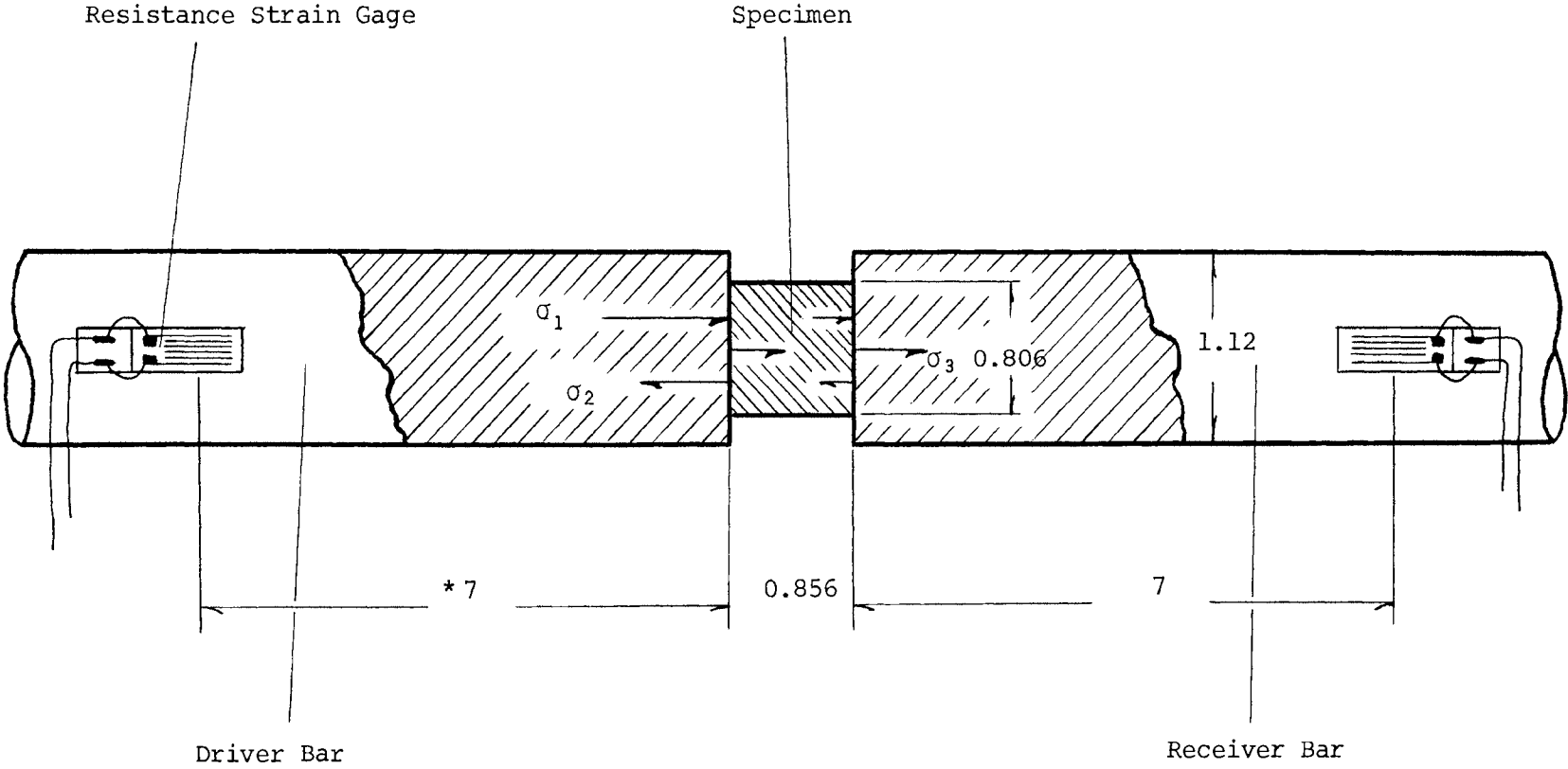


Figure 20. Sketch of Specimen Area Showing Symbols Used.

A schematic diagram showing the internal reactions which occur in the split Hopkinson bar apparatus is shown in figure 21. Characteristic effects as the waves progress down the bar are noted in each of the sketches which are listed alphabetically in order of increasing time. For the particular case shown the driver and receiver bar are of equal length ($L_D = L_R$) and the projectile is half as long ($L_B = \frac{1}{2}L_D$). The impact velocity of the projectile is v_0 while the remainder of the bar is initially at rest. The driver bar, receiver bar and projectile are of the same material and have the same diameters.

Part (a) (figure 21) shows the situation in which the impactor initially makes contact with the driver bar. In (b), a compressional wave is propagated in both directions from the impact interface until in (c) the wave reaches the free end of the projectile. The velocity in the compressed region is $\frac{1}{2}v_0$ and stress in the region is given from equation (4) as $\sigma = \frac{1}{2}\rho_D C_D v_0$. Explanations of these relationships are given in later paragraphs. In (d), a tensile wave reflects at the free boundary of the projectile and the compressional wave in the driver bar reaches the position where strain gages are located. In (e), the driver bar is compressed throughout its length and the reflected wave reaches the interface between the projectile and the driver bar. The projectile is now at rest since all of its momentum has been transferred to the driver bar. In (f), the wave reflected at the interface between the driver bar and the specimen reaches the strain gages on the driver bar. In (g), the transmitted wave through the specimen reaches the strain gages on the receiver bar. There will be other reflections as a result of mismatch of impedance between the specimen and receiver bars but these have been omitted for clarity.

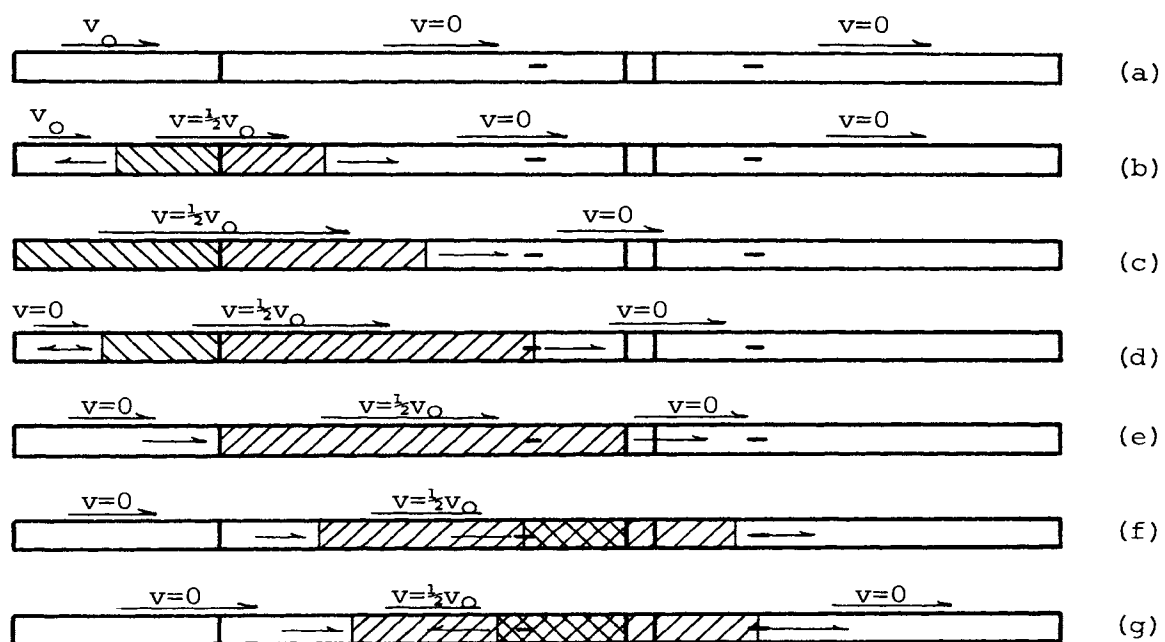


Figure 21. Diagram Showing Stress Wave Propagation in Split Hopkinson Bar.

The analytical relations which govern the Hopkinson bar are derived below. The desired output is stress, strain and strain rate as a function of time within the specimen.

The velocity of one-dimensional stress waves in a prismatic bar is

$$c = \sqrt{\frac{E}{\rho}} \quad (1)$$

where

E = Young's modulus

ρ = density .

The particle velocity in a compressed region undergoing one-dimensional stress loading can be derived using momentum methods. For example, figure 21 (b) shows a compression stress wave which has propagated through half the length of the projectile. From the conservation of momentum

$$L_B \rho_B A_B v_0 = \frac{1}{2} L_B \rho_B A_B v_0 + \frac{1}{2} L_B \rho_B A_B v + \frac{1}{4} L_D \rho_D A_D v$$

and since

$$L_D = 2L_B, \rho_D = \rho_B \text{ and } A_D = A_B$$

$$\frac{1}{2} L_B \rho_B A_B v_0 = L_B \rho_B A_B v$$

and finally

$$v = \frac{1}{2} v_0 \quad (2)$$

The symbols A_B and A_D represent the cross-sectional area of the projectile and driver bar respectively and in this case have been assumed to be equal. The respective densities ρ_B and ρ_D are also equal.

As assumed previously, stresses in the driver and receiver bars remain in the linear elastic range throughout the test. A step pulse of constant amplitude is generated as a result of the impact of the

projectile with the driver bar. In this case the impulse-momentum relation can be used in the form

$$mv - mv_0 = \int_0^t Fdt \quad . \quad (3)$$

For the above equation, mv is the momentum of the projectile at time t , mv_0 is the initial momentum of the projectile and F is the applied force, constant in this case. Considering the driver bar as a system in which the initial momentum is zero and a velocity v is acquired in the stressed region after impact, the momentum after a time dt is

$$\rho AvdL$$

where dL represents the distance the wave propagates in the time dt . The impulse is Fdt or σAdt where σ is the applied stress. Equating the two quantities gives

$$AvdL = \sigma Adt$$

or

$$\sigma = \rho v \frac{dL}{dt} \quad .$$

The wave velocity C is dL/dt so

$$\sigma = \rho Cv \quad (4)$$

for a simple impact of the type considered. The stresses then are easily determined once the particle velocities are known. With this in mind the stress in the compressed region of the driver bar can be evaluated from the initial impact velocity of the projectile with the equation

$$\sigma_1 = \frac{1}{2} \rho C v_0 \quad (5)$$

The strain-time histories in the two pressure bars are recorded by means of resistance strain gage measurements. The incident loading strain is termed, ϵ_1 , the reflected strain, ϵ_2 , and the transmitted strain, ϵ_3 . Compressive stress and strain are positive and the relations given below are derived for the case where the impedance of the specimen is less than the impedance of the driver and receiver bars. The computer program was also written with these conventions. The reflected stress σ_2 is tensile and accordingly has been given a negative sign in the equation.

The stresses in the system are obtained from the strain gage readings by means of the following equations,

$$\begin{aligned}\sigma_1(t) &= E_D \epsilon_1(t) \quad , \\ \sigma_2(t) &= E_D \epsilon_2(t) \quad , \\ \sigma_3(t) &= E_R \epsilon_3(t) \quad .\end{aligned}\tag{6}$$

where

$$\begin{aligned}\sigma_1 &= \text{incident stress} \\ \sigma_2 &= \text{reflected stress} \\ \sigma_3 &= \text{transmitted stress} \\ E_D &= \text{elastic modulus of the driver bar} \\ E_R &= \text{elastic modulus of the receiver bar} .\end{aligned}$$

Forces must balance at the two specimen interfaces. Therefore at the front face

$$\sigma_{SI} A_S = (\sigma_1 - \sigma_2) A_D$$

from which

$$\sigma_{sI} = \frac{(\sigma_1 - \sigma_2)A_D}{A_S} .$$

At the interface with the receiver bar

$$\sigma_{sII}A_S = \sigma_3A_R$$

and

$$\sigma_{sII} = \frac{\sigma_3A_R}{A_S} .$$

The symbols σ_{sI} and σ_{sII} refer to stresses on the front and back faces of the specimen respectively. Also, A_D and A_R are the cross sectional areas of the driver and receiver bar which in this work are assumed equal.

The average stress in the specimen is therefore

$$\sigma_{AVG} = \frac{\sigma_{sI} + \sigma_{sII}}{2}$$

or

$$\sigma_{AVG} = \frac{(\sigma_1 - \sigma_2 + \sigma_3)A_D}{2A_S} \quad (7)$$

All of these stresses, σ_1 , σ_2 , and σ_3 , are assumed to be functions of time.

The velocities of the front and back faces of the specimen, V_I , V_{II} , respectively, are given by

$$V_I(t) = \frac{\sigma_1(t) + \sigma_2(t)}{\rho_D C_D} \quad (8)$$

and

$$V_{II}(t) = \frac{\sigma_3(t)}{\rho_R C_R} ; \quad (9)$$

where

ρ_D = density of the driver bar

ρ_R = density of the receiver bar

C_D = wave velocity in the driver bar

C_R = wave velocity in the receiver bar .

In this work

$$\rho_D = \rho_R$$

and $C_D = C_R$.

The average strain rate in the specimen is

$$\dot{\epsilon}_s(t) = \frac{V_I(t) - V_{II}(t)}{L_S} \quad . \quad (10)$$

Substituting equations (8) and (9) into equation (10) gives

$$\dot{\epsilon}_s(t) = \frac{\sigma_1(t) + \sigma_2(t) - \sigma_3(t)}{\rho_D C_D L_S} \quad . \quad (11)$$

The average strain in the specimen is obtained by integrating with respect to time to give

$$\epsilon_s(t) = \int_0^t \dot{\epsilon}_s(t) dt \quad . \quad (12)$$

Equations (6) through (12) have been utilized in the computer program listed in Appendix A.

VI. PARTICULAR TEST RESULTS

For the purpose of verifying the design of the split Hopkinson bar tests were performed on specimens of 1100-0 aluminum. Many people have tested this particular material because of its strain rate sensitivity. In a sense it has become a standard for the Hopkinson bar experiment.

Several 1100 aluminum specimens, 0.5 in. in diameter and various lengths up to a maximum of 0.5 in., were heat treated in a metallurgical furnace to obtain 1100-0 material. The furnace was maintained at a temperature of 560 degrees centigrade for 17 hours. The specimens were then removed and cooled in ambient air to complete the annealing process. Tests were then conducted with the split Hopkinson bar and results were compared with data reported by Lindholm and Yeakley (6). (See Appendix B) Sufficient correlation was obtained to establish reasonable confidence in the design of the bar and the computer program used to analyze the data.

Following proof tests on aluminum, a particular gypsum plaster material called "Hydrostone"* was selected to be studied in the split Hopkinson bar. This material is a plaster which is of interest because in the past it has been used as a modeling material to simulate rock. It was of interest to determine its dynamic response and later to perform dynamic tests with embedded gages.

Hydrostone is delivered as a powder in bags and is mixed with water in some given ratio when it is to be used. Special care during preparation is required to reduce bubble formation in the mix. Experience has shown that fewer bubbles are introduced in thin mixtures, however, the strength also decreases with increasing water content.

* Manufactured by U.S. Gypsum Company

The procedure followed was to prepare the mixture in an open container with a ratio of Hydrostone to water of 2.49 to 1 by weight. The water and plaster were mixed by hand and the container was mounted on a mechanical shaker and vibrated for approximately one minute. The bubbles were then removed from the surface and the material was poured into cylindrical plastic molds which were inclined at approximately 15 degrees with the vertical. Also prepared was a 4 in. cubic block to be used in the isotropy test which is described in later paragraphs.

The cylinders as cast were $1\frac{1}{2}$ in. in diameter and 8 in. long from which the ends were cut off to give a 4 in. test piece for the static compression tests. Strain gages (Dentronics type 23NC13) were installed on the specimen as shown in figure 22. Static uniaxial compression tests were then performed to obtain stress strain data in compression and the results are shown in figure 23. From this test the elastic modulus was determined to be 1.65×10^6 psi and the yield/failure stress to be 4810 psi. Other tests showed the unit weight to be 0.0564 lb/in^3 .

In order to check the isotropy and homogeneity of cast Hydrostone, a 4 in. cube of the material was subjected to an ultrasonic test. In this experiment an ultrasonic signal is propagated across the specimen and the time required for transit is noted from an oscilloscope trace. The pulse travel time through 4.00 in. of the Hydrostone was found to be 33.5 μsec . and further, the same result was obtained for three orthogonal directions. Based on these tests it was assumed that the cast material was isotropic and homogeneous.

Hopkinson bar specimens were cast in a mold which had a diameter of 0.86 in. and the samples were later cut to various lengths approximately equal to the diameter. The faces of the specimens were ground

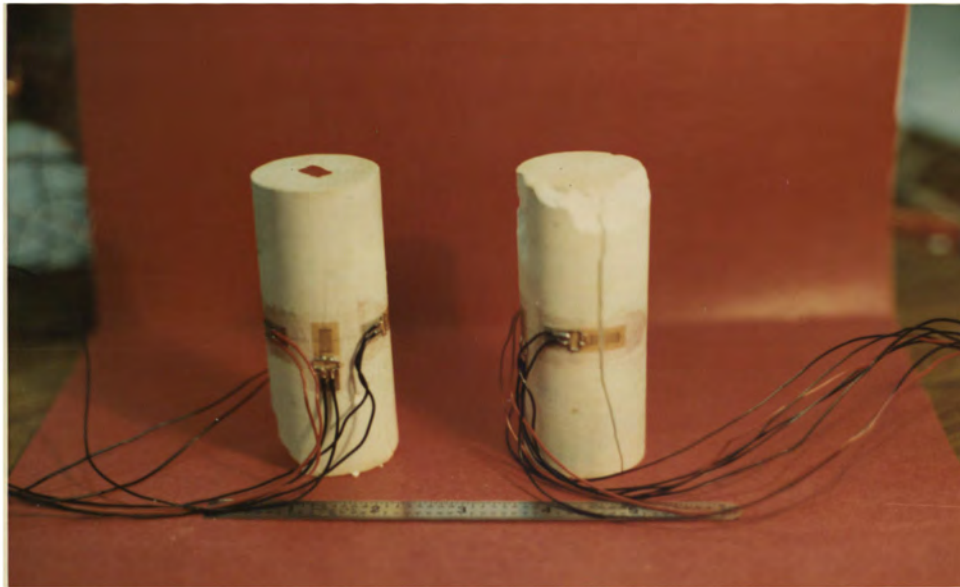


Figure 22. Compressive Failure of Hydrostone Specimens
in a Universal Test Machine.

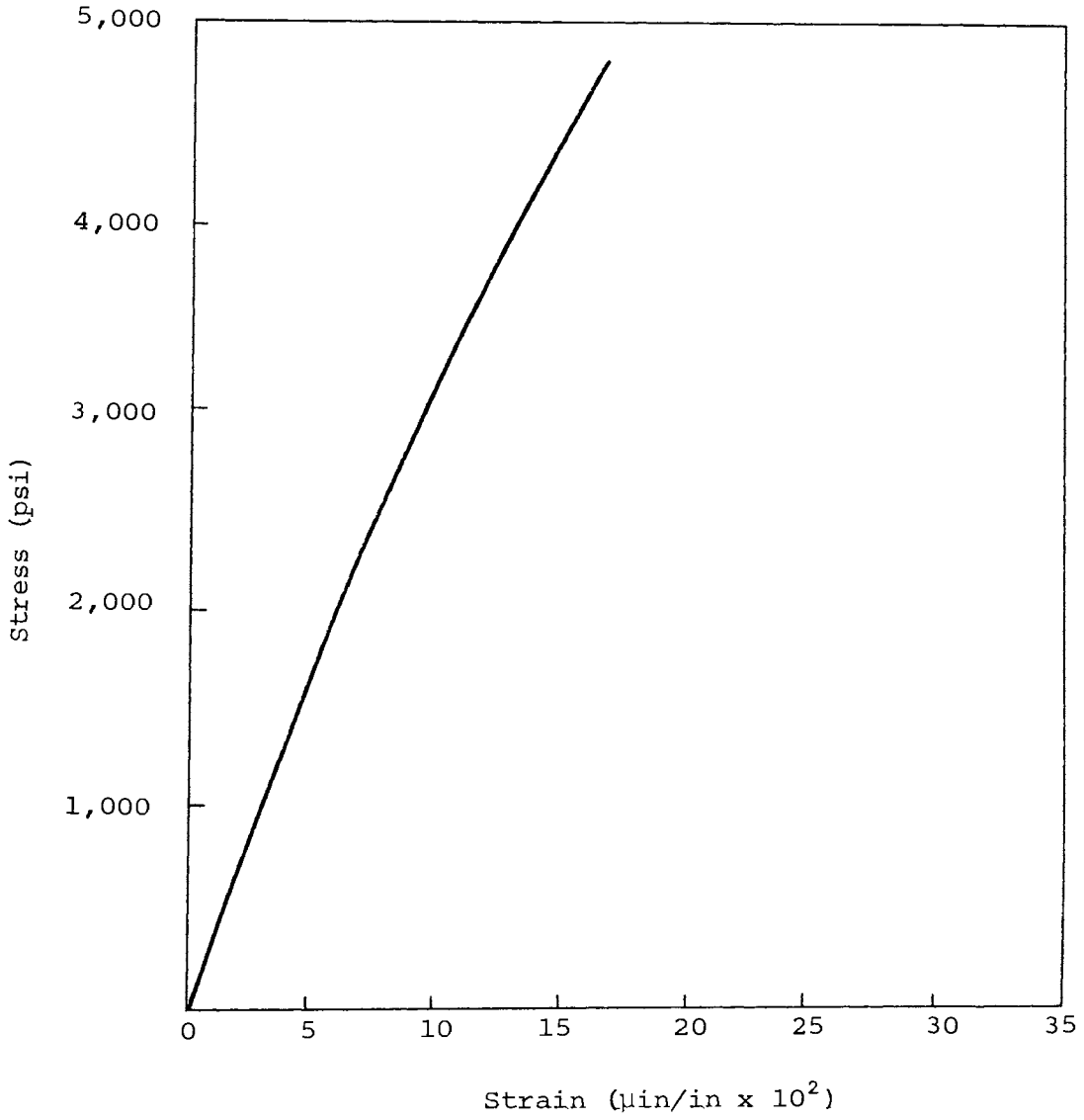


Figure 23. Static Stress Strain Diagram for Hydrostone.

flat and true on an automatic surface grinder. Several samples were tested with length as a variable so that the strain rate could be varied.

Results of dynamic tests are shown in figure 24 in which stress versus strain and strain rate are plotted. The static compressive breaking strength was found to be approximately 4810 psi and this is indicated on the graph. The curve for strain rate of approximately 40/sec. and 60/sec. is also sketched through the experimental data points. It is seen that the material exhibits strain rate sensitivity, however, further testing is needed to properly fill out the curves. The reader is warned not to expect rocks and rock-like materials to perform as do ductile metals.

A computer program was written to analyze data from the Hopkinson experiment. Input quantities in this code are incident strain, reflected and transmitted strains which are read from photographs of the oscilloscope traces. One of the key parameters calculated is the percentage difference in stress across the specimen length. When this difference is ± 5 percent, the computed values were assumed to be valid. A listing of the computer program is included in Appendix A.

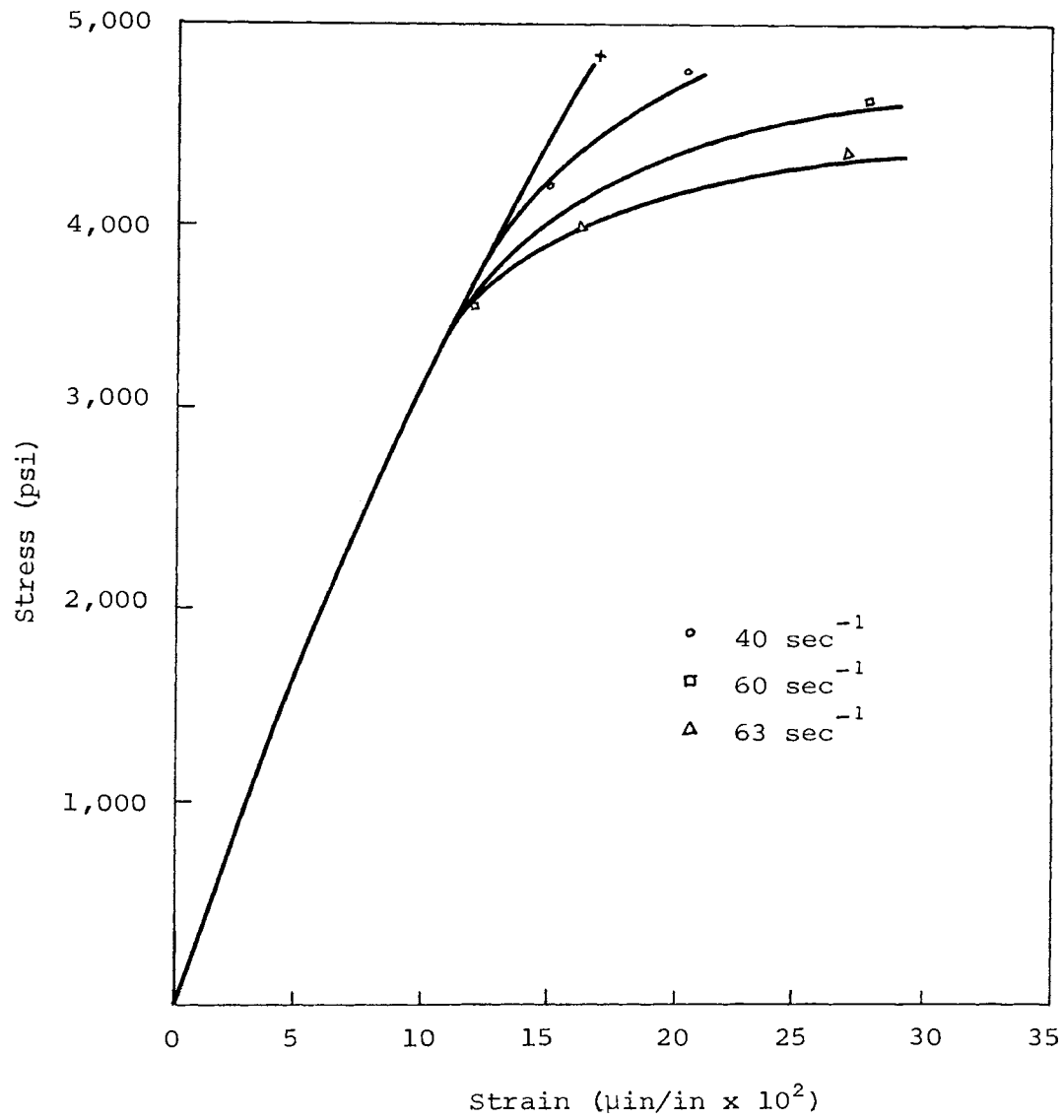


Figure 24. Preliminary Test Data on Hydrostone.

VII. CONCLUSIONS AND RECOMMENDATIONS

The concern of this paper has been the design and construction of a split Hopkinson bar. Analytical methods useful in analyzing strain readings from the bar have been presented along with test data on one material. A computer program has been developed to aid in the calculation of desired quantities.

Tests on 1100-0 aluminum have indicated that the instrumentation and method of analysis give reasonable results. Experience has shown that satisfactory control of the projectile impact velocity is exercised with the air accumulator and solenoid switch arrangement. The system will produce velocities in excess of 200 in/sec for the projectile described in the report.

The electronic systems have also proven to be excellent for strain measurement, triggering and display. With the bridge and amplifier units employed, dynamic strains of the order of $10 \mu\text{in/in}$ can be recorded and discerned.

Preliminary testing was conducted on a plaster called Hydrostone. This material is often used for rock modelling purposes because its mechanical behavior simulates rock in many respects and because strain gages can be embedded within it to allow internal strains to be sensed. Hydrostone samples were prepared and tested statically in a universal testing machine to determine stress-strain curves. Following this, ultrasonic tests were conducted and it was deduced that the material is isotropic and homogeneous. Finally the Hopkinson bar was used to produce strain rate information which has been included.

Recommendations for future work:

1. The present study should be extended to include two-dimensional effects in impacts. Computer programs are available which could be adapted to problems of this type once the material constitutive equations are known. Specific areas which should be studied are impacts between bars of unequal diameters, frictional effects on the plane of impact and the general problem of internal strain prediction and measurement.
2. More testing should be conducted with Hydrostone to extend the preliminary data presented in this report.
3. The Hopkinson bar should be adopted and used to measure dynamic tensile and compressive properties of rocks.

VIII. APPENDIX A

Stress, strain and strain rate of the specimen

The UMR IBM/360 digital computer is used to calculate stress, strain and strain rate as a function of time. The computer program is given as follows:

```

C
C
C   HOPKINSON BAR COMPUTER CODE
C
C
C   S1 = INCIDENT STRESS PULSE (PSI)
C   S2 = REFLECTED STRESS PULSE (PSI)
C   S3 = TRANSMITTED STRESS PULSE (PSI)
C   SAVG = AVERAGE STRESS IN THE SPECIMEN (PSI)
C   SF = STRESS AT THE FRONT FACE OF THE SPECIMEN (PSI)
C   E1 = INCIDENT STRAIN IN THE DRIVER BAR (MICROIN/IN)
C   E2 = REFLECTED STRAIN IN THE DRIVER BAR (MICROIN/IN)
C   E3 = STRAIN IN THE RECEIVER BAR (MICROIN/IN)
C   ES = STRAIN IN THE SPECIMEN (MICROIN/IN)
C   EDOT = STRAIN RATE IN SPECIMEN (1/SEC)
C   C = WAVE SPEED IN THE DRIVER BAR (IN/SEC)
C   T = TIME IN MICROSECONDS
C   D = DELAY TIME ACROSS SPECIMEN - MICROSECONDS
C   INPUT DATA
C   Y1 = MODULUS OF THE DRIVER BAR (PSI)
C   Y2 = MODULUS OF THE RECEIVER BAR (PSI)
C   LS = LENGTH OF SPECIMEN (IN)
C   AD = AREA DRIVER BAR (IN**2)
C   AS = AREA SPECIMEN (IN**2)
C   N = NUMBER OF DATA POINTS
C   SPWT = SPECIFIC WEIGHT OF DRIVER BAR (LB/IN**3)
C   DELT = TIME INCREMENT IN MICROSECONDS OF INPUT DATA
C   CS = SPECIMEN WAVE SPEED (IN/SEC)
C   DD = DIA. OF DRIVER BAR (IN)
C   DS = DIA. OF SPECIMEN (IN)
C   YS = MODULUS OF SPECIMEN (PSI)
C   SPWTS = SPECIFIC WEIGHT OF SPECIMEN (LB/IN**3)
C   N = NO. OF DATA POINTS
C   ALL INPUT STRAINS ARE IN MICROINCHES/IN
C
C   GF = GAGE FACTOR
C
C
C
C   STRAIN READINGS ARE CORRECTED ACCORDING TO DATA FROM
C   MICRO MEASUREMENTS CHARTS FOR NONLINEAR STRAIN BRIDGE RELATION.

```

C
C
C
C
C
C
C
C
C
C

SO LONG AS TWO ACTIVE GAGES ON EITHER SIDE OF THE DRIVER BAR
ARE BEING AVERAGED, THE CORRECTION FACTOR EQUATION IS CORRECT.

```

        DIMENSION T(500),E1(500),E2(500),S1(500),S2(500),S3(500)
1,EDOT(500),SAVG(500),SF(500),E3(500),E4(500),E3C(500)
        DIMENSION PD(500)
        DIMENSION S(500)
        REAL*4 LS
        READ(1,60)Y1,Y2,DD,SPWT,GF
60      FORMAT(2E10.4,3F10.4)
        READ(1,61)YS,DS,SPWTS,LS,EEL, RT
61      FORMAT(E10.4,5F10.4)
        READ(1,62)N,DELT
62      FORMAT(I5,F10.3)
        IF(RT - DELT) 5,5,7
5        E1(1) = 0
        DO 8 I=2,N
8        E1(I) = EEL
        GO TO 9
7        I = 1
150     DEL1 = DELT * I
        IF(DEL1-RT)120,130,140
120     I = I + 1
        GO TO 150
130     M = I + 1
        DO 160 K=1,M
        L = K - 1
160     E1(K) = (EEL/RT) * DELT * FLOAT(L)
        L = M + 1
        DO 170 K=L,N
170     E1(K) = EEL
        GO TO 9
140     CONTINUE
        DO 180 K=1,I
        L = K - 1
180     E1(K) = (EEL/RT) * DELT * FLOAT(L)
        L = I + 1
        DO 190 K=L,N
190     E1(K) = EEL
9        CONTINUE
        RHOS=SPWTS/386.
        AS=.7854*DS**2
        AD=.7854*DD**2
        CS=SQRT(YS/RHOS)
        A=AD/(2.*AS)
        RHO = SPWT/386.
        C=SQRT(Y1/RHO)

```

```

B=RHO*C*LS
WRITE(3,35)
35  FORMAT(1H1)
    WRITE(3,63)
63  FORMAT(//,'DRIVER MODULUS'5X' TRANS MODULUS'5X'DRIVER DIA(IN.)'5X'
1DRIVER SP. WGT',5X'WAVE SPEED',5X,'GAGE FACTOR',5X,
1'RISE TIME(MCS) ',//)
    WRITE(3,64)Y1,Y2,DD,SPWT,C,GF,RT
64  FORMAT(1PE14.3,E18.3,OPF20.4,F19.4,1PE15.3,OPF16.2,OPF19.3)
    WRITE(3,65)
65  FORMAT(//,' SPECIMEN MODULUS'5X'SPEC.DIA.(IN.)'5X'SPEC.SP. WGT'5X
1'SPEC LENGTH',5X,'SPEC WAVE SPEED',//)
    WRITE(3,66)YS,DS,SPWTS,LS,CS
66  FORMAT(1PE16.3,OPF19.4,F15.4,F16.4,1PE18.3)
    WRITE(3,67)
67  FORMAT(//,' NO. OF DATA POINTS'5X'TIME INCREMENT(MICROSEC) ',//)
    WRITE(3,68)N,DELT
68  FORMAT(I9,F23.3)
    READ(1,11)(T(I),E2(I),E3(I),I=1,N)
11  FORMAT(3F10.3)
    WRITE(3,899)
899  FORMAT(//,' RAW UNCALIBRATED DATA CORRECTED FOR RISE TIME',//)
    WRITE(3,901)
901  FORMAT(//' INTERGER'5X'TIME(MCS)'5X'STRAIN 1'5X'STRAIN 2'5X'STRAIN
1 3'//)
    WRITE(3,902)(I,T(I),E1(I),E2(I),E3(I),I=1,N)
902  FORMAT(I5,4F15.6)
    CALIB = 1.0
    DO 1200 I=1,N
    E1(I)=E1(I)*CALIB
    E2(I)=E2(I)*CALIB
1200 E3(I)=E3(I)*CALIB
    WRITE(3,36)
36  FORMAT(//,'RAW CALIBRATED DATA'//)
    WRITE(3,37)
37  FORMAT(//,' INTERGER',5X'TIME(MICROSEC)',5X'INCID STRAIN(MICROIN/IN)
1)'5X'REFL STRAIN(MICROIN/IN)'5X'TRANS STRAIN(MICROIN/IN)'//)
    WRITE(3,38)(I,T(I),E1(I),E2(I),E3(I),I=1,N)
38  FORMAT(I5, F14.2,F29.6,F28.6,F29.6)
    DO 12 I=1,N
    E1(I)=E1(I)/1.E6
    E2(I)=E2(I)/1.E6
12  E3(I)=E3(I)/1.E6
    WRITE(3,400)
400  FORMAT(//,' RAW DATA CORRECTED FOR NONLINEAR STRAIN BRIDGE '
1'RELATION',//)
    DO 401 J=1,N
    E1(J)=E1(J)*(1.+(GF*E1(J))/(2.-GF*E1(J)))
    E2(J)=E2(J)*(1.+(GF*E2(J))/(2.-GF*E2(J)))
401  E3(J)=E3(J)*(1.+(GF*E3(J))/(2.-GF*E3(J)))
    WRITE(3,402)
402  FORMAT(//,' INTEGER',5X'TIME(MICROSEC)',5X'INCID STRAIN(MICROIN/IN)
1)'5X'REFL STRAIN(MICROIN/IN)'5X'TRANS STRAIN(MICROIN/IN)'//)

```

```

WRITE (3,88) (I,T(J),E1(J),E2(J),E3(J),J=1,N)
88  FORMAT(I5, F14.2,F29.6,F28.6,F29.6)
DO 403 I=1,N
S1(I)=Y1*E1(I)
S2(I)=Y1*E2(I)
S3(I)=Y2*E3(I)
SAVG(I)=(S1(I)-S2(I)+S3(I))*A
403  EDOT(I)=(S1(I)+S2(I)-S3(I))/B
M=N-1
WRITE (3,14)
14  FORMAT(//,' INTEGER'5X'TIME (MCS)'5X'STRESS-INCID (PSI)'5X'STRESS-RE
1FL(PSI)'5X'STRESS-TRANS (PSI)')//)
WRITE (3,15) (I,T(I),S1(I),S2(I),S3(I),I=1,M)
15  FORMAT(I5,F17.2,F22.2,F21.2,F22.2)
DELT1=DELT*1.E-6
SUM=0.
DO 13 I=1,M
DSUM=((EDOT(I+1)+EDOT(I))/2.)*DELT1
SUM=SUM+DSUM
13  E4(I)=SUM
WRITE (3,28)
28  FORMAT(1H1)
WRITE (3,29)
29  FORMAT(' SPECIMEN CONDITIONS')
WRITE (3,16)
16  FORMAT(//' INTEGER'5X'TIME (MICROSEC)'10X'STRESS (PSI)'5X'STRAIN (IN/
1LIN)'5X'STRAIN RATE (PER SEC)')//)
WRITE (3,17) (I,T(I),SAVG(I),E4(I),EDOT(I),I=1,M)
17  FORMAT(I5,F22.2,F21.2,F18.6,F25.2)
WRITE (3,590)
590  FORMAT(//' INTEGER'5X'TIME (MCS)'5X'STRESS-FRONT'5X'STRESS-BACK'5X'
1STRESS-DIFF %'5X'STRAIN'5X'STRAIN RATE'5X'STRESS',//)
DO 1231 I=1,N
SF(I)=ABS(S1(I)-S2(I))
IF(SF(I) .LE. 0.005) GO TO 510
PD(I)=((SF(I)-S3(I))/SF(I))*100.
WRITE (3,55) I,T(I),SF(I),S3(I),PD(I),E4(I),EDOT(I),SAVG(I)
55  FORMAT(I5,2F17.2,F16.2,F14.2,4X,F11.6,F16.2,F11.2)
GO TO 1231
510  WRITE (3,56) I,T(I),SF(I),S3(I),E4(I),EDOT(I),SAVG(I)
56  FORMAT(I5,2F17.2,F16.2,10X'-----',4X,F11.6,F16.2,F11.2)
1231  CONTINUE
STOP
END
/ DATA

```

APPENDIX B

Particular test results using 1100-0 aluminum

Curves are from a paper by Lindholm and Yeakley(6).

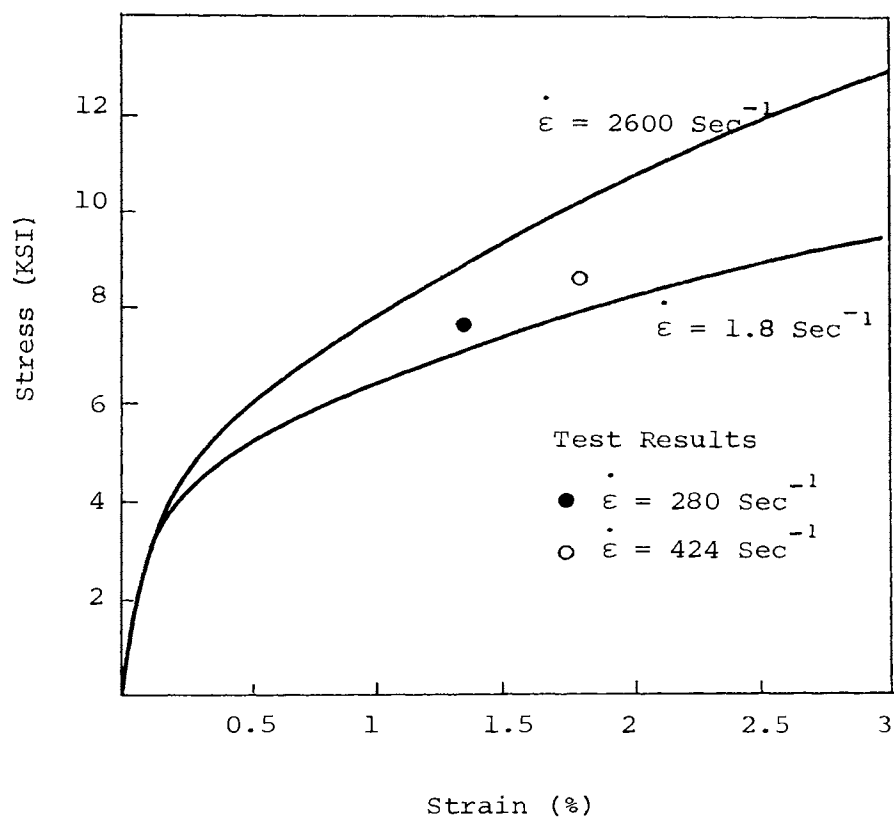


Figure 25. Stress, Strain and Strain Rate Test Results for 1100-0 Aluminum.

IX. BIBLIOGRAPHY

1. McQUEEN, R.G. and MARSH, S.P., "Equation of State for Nineteen Metallic Elements from Shock-Wave Measurements to Two Megabars", JOURNAL OF APPLIED PHYSICS, Vol. 31, No. 7, p. 1253, 1960.
2. HOPKINSON, B., "A Method of Measuring the Pressure Produced in the Detonation of High Explosives or by the Impact of Bullets", PHILOSOPHICAL TRANSACTIONS, Vol. 213A, p. 437, 1914.
3. DAVIES, R.M., "A Critical Study of the Hopkinson Pressure Bar", PHILOSOPHICAL TRANSACTIONS, Vol. 240A, p. 375, 1948.
4. KOLSKY, H., "An Investigation of the Mechanical Properties of Materials at Very High Rates of Loading", PROCEEDINGS OF THE PHYSICAL SOCIETY, B, Vol. LXII, p. 676, 1949.
5. MAIDEN, C.J., and GREEN, S.J., "Compressive Strain-Rate Test on Six Selected Materials at Strain Rates from 10^{-3} to 10^4 in/in/sec", JOURNAL OF APPLIED MECHANICS, Vol. 33, Series E, No. 3, p. 496, 1966.
6. LINDHOLM, U.S. and YEAKLEY, L.M., "High Strain-Rate Testing: Tension and Compression", EXPERIMENTAL MECHANICS, Vol. 8, p. 1, 1968.
7. RAND, J.L. and JACKSON, J.W., "The Split Hopkinson Pressure Bar", BEHAVIOR OF DENSE MEDIA UNDER HIGH DYNAMIC PRESSURES, Gordon and Breach, New York, 1967.
8. RICKETTS, T.E. and GOLDSMITH, W., "Dynamic Properties of Rocks and Composite Structural Materials", INTERNATIONAL JOURNAL OF ROCK MECHANICS AND MINING SCIENCES, Vol. 7, No. 3, p. 315, 1970.

X. VITA

Woosoon Bai was born on February 2, 1940, in Korea. He received his primary and secondary education in Seoul, Korea. He received a Bachelor of Science Degree from the Department of Mechanical Engineering at In-Ha Institute of Technology in December, 1964, in Inchon, Korea.

He has been enrolled in the Graduate School of the University of Missouri - Rolla since September 1968. He has been associated with the Rock Mechanics and Explosives Research Center - U.M.R. as a graduate research assistant since September 1969.